Polar Biology
https://doi.org/10.1007/s00300-019-02494-4

ORIGINAL PAPER

Spatio-temporal distribution of polar cod (*Boreogadus saida*) and saffron cod (*Eleginus gracilis*) early life stages in the Pacific Arctic

Cathleen D. Vestfals[1] · **Franz J. Mueter**[2] · **Janet T. Duffy-Anderson**[3] · **Morgan S. Busby**[3] · **Alex De Robertis**[3]

Received: 24 September 2018 / Revised: 15 March 2019 / Accepted: 18 March 2019

Abstract

Polar cod (*Boreogadus saida*) and saffron cod (*Eleginus gracilis*) are key fishes in the Arctic marine ecosystem, serving as important trophic links between plankton and apex predators, yet our understanding of their life histories in Alaska's Arctic is extremely limited. To improve our knowledge about their early life stages (ELS), we described the spatial and temporal distributions of preflexion larvae to late juveniles (to 65 mm in length) in the Chukchi and western Beaufort seas based on surveys conducted between 2004 and 2013, and examined how their abundances varied in response to environmental factors. Species-specific differences in habitat use were found, with polar cod having a more offshore and northern distribution than saffron cod, which were found closer inshore and farther south. Polar cod preflexion and flexion larvae were encountered throughout the sampling season across much of the shelf, which suggests that spawning occurs over several months and at multiple locations, with Barrow Canyon potentially serving as an important spawning and/or retention area. Polar cod ELS were abundant at intermediate temperatures (5.0–6.0 °C), while saffron cod were most abundant at the highest temperatures, which suggests that saffron cod may benefit from a warming Arctic, while polar cod may be adversely affected. This research provides new insights into how environmental variability influences the distribution and abundance of gadids in the Pacific Arctic and advances our understanding of the habitats occupied by these key forage species during their first few months of life.

Keywords *Boreogadus saida* · *Eleginus gracilis* · Early life stages · Distribution · Chukchi Sea · Beaufort Sea

Introduction

Polar cod (*Boreogadus saida*) and saffron cod (*Eleginus gracilis*) are key fishes in the Pacific Arctic marine ecosystem, serving as important trophic links between plankton and apex predators such as piscivorous seabirds, marine mammals, and humans (Bradstreet 1986; Whitehouse 2011). While the basic biology and life history of these two species is relatively well understood at the species level (Wolotira 1985; Bradstreet 1986), much less is known about their ecology (e.g., abundance, distribution, migrations, and patterns of habitat use) in Alaska's Arctic. Given their important ecological role, there is a need to characterize the habitat these species occupy, particularly during their early life stages (ELS). Information about the seasonal and spatial distributions of ELS is important for identifying habitat critical to spawning and development, characterizing the dispersal of eggs and larvae from spawning locations to juvenile nursery habitats, and understanding how environmental variability can alter connectivity between these habitats, which can potentially affect recruitment and population dynamics.

Polar cod is the most abundant and ubiquitous fish species in the Arctic, with a circumpolar distribution extending from the Arctic Basin onto the surrounding shelves and into the marginal seas (Bradstreet 1986; Scott and Scott 1988;

Electronic supplementary material The online version of this article (https://doi.org/10.1007/s00300-019-02494-4) contains supplementary material, which is available to authorized users.

✉ Cathleen D. Vestfals
cdvestfals@alaska.edu

[1] Hatfield Marine Science Center, University of Alaska Fairbanks, College of Fisheries and Ocean Sciences, 2030 S.E. Marine Science Drive, Newport, OR 97365, USA

[2] University of Alaska Fairbanks, College of Fisheries and Ocean Sciences, 17101 Point Lena Loop Road, Juneau, AK 99801, USA

[3] Alaska Fisheries Science Center, National Marine Fisheries Service, NOAA, 7600 Sand Point Way N.E., Seattle, WA 98115, USA

Mecklenburg et al. 2018). Polar cod are known to undertake extensive migrations between their summer feeding and winter spawning grounds, moving southward in the fall and returning northward in the spring (Baranenkova et al. 1966; Ponomarenko 1967, 1968; Gjøsæter 1973). Spawning locations in Alaska's Arctic are currently unknown, although in the Siberian Arctic it occurs along the Chukotka Peninsula south to the Gulf of Anadyr (Sunnanå and Christiansen 1997). Spawning occurs in areas near the ice edge and/or under ice cover from November to March (Baranenkova et al. 1966; Ponomarenko 2000), with peak spawning in January and February (Craig et al. 1982). Spawning takes place close to the surface (Shleinik 1973 and Yudanov 1976 in Ponomarenko 2000), though it may also occur near the seafloor (Ponomarenko 1968; Geoffroy et al. 2011). A number of nearshore, shallow spawning grounds are thought to exist in the North American and Siberian Arctic (Craig et al. 1982; Thanassekos and Fortier 2012; Logerwell et al. 2015).

Polar cod eggs are pelagic and buoyant, rising to the ice–water interface after they are spawned (Yudanov 1976; Graham and Hop 1995; Ponomarenko 2000). Eggs develop under ice cover or in areas that have recently become ice-free (Rass 1968), with development times ranging from 35 days at 1.5 °C (Aronovich et al. 1975) to 77–79 days at − 1.5 °C in the laboratory (Altukhov 1981). Hatching occurs as early as December in regions warmed by large freshwater inputs and as late as August in colder regions (Bouchard and Fortier 2011), with peak hatching in May and June, coinciding with the timing of ice break up (Yudanov 1976; Bouchard and Fortier 2008). Laboratory studies have shown that larvae are surface-oriented, at least for the first few months of life (B. Laurel, National Oceanic and Atmospheric Administration (NOAA), personal communication). In the Barents Sea, newly hatched larvae were found within 5 m of the surface and moved deeper as they developed (Borkin et al. 1986). In late summer, pelagic juveniles descend from the surface layers to deeper in the water column between 30 and 55 mm in length (Matarese et al. 1989; Ponomarenko 2000; Bouchard and Fortier 2011), but most often between 35 and 45 mm (ICES CM 1983, 1985, 1986, 1987, 1988).

Saffron cod have an Arctic-boreal Pacific distribution and are widely distributed in nearshore regions of the North Pacific from the Korean Peninsula to southeast Alaska, and to Dease Strait in the Canadian Arctic (Mecklenburg et al. 2002). Although typically marine, they can live in brackish waters for extended periods of time, particularly as juveniles (Wolotira 1985). Spawning typically occurs in January and February, but can extend from late December through the end of March depending upon the region and severity of winter conditions (Pokrovskaya 1960; Bond 1982). In relatively mild winters, peak spawning occurs later and is often prolonged, compared to cold winters, when spawning begins earlier and peak activity occurs over a shorter period (Wolotira 1985). Saffron cod spawn demersally under ice in shallow (2–10 m), nearshore areas with sandy-pebbly substrate, and high salinity waters under strong tidal influence (Morrow 1980; Fechhelm et al. 1985; Wolotira 1985; Johnson 1995; Mecklenburg et al. 2002).

Saffron cod eggs are demersal, (slightly) adhesive, and are capable of successful development under ice at sub-zero temperatures (Berg 1949; Wolotira 1985). Temperature-dependent egg development ranges from 90 days at − 1 °C to 33 days at 5 °C in the laboratory (B. Laurel, NOAA, personal communication). Peak hatching occurs in April and May, prior to the warming of coastal waters in the Arctic and northern Pacific, though it occurs later farther south (Wolotira 1985). Newly hatched larvae spend between 2–3 months in the plankton before descending to the bottom in mid-summer, between 39 and 56 mm in length in the Pacific and 55 and 60 mm in the Arctic (Wolotira 1985), though larger age-0 fish can still be found in surface waters in late summer (Eisner et al. 2012).

The Arctic is undergoing rapid, unprecedented environmental change. Air temperatures have increased by 3.5 °C since the beginning of the twentieth Century (Richter-Menge et al. 2016) and in the Beaufort and Chukchi seas, monthly surface air temperature anomalies that exceed 6 °C are now frequent occurrences (Wood et al. 2015). The Chukchi Sea is experiencing one of the largest warming trends of any marine environment (Richter-Menge et al. 2016). In addition to large reductions in sea-ice concentration (Comiso et al. 2008), sea-ice extent and duration have declined dramatically, with earlier spring ice retreat and delayed fall ice formation shortening the period of ice cover by ~ 3 months (Stammerjohn et al. 2012). It is unclear how reduced ice cover, earlier ice melt, and greater freshwater input associated with warming in the Arctic will impact species like polar cod and saffron cod, which spend a large portion of their lives under the ice. Recent laboratory studies have shown that polar cod have a cold-adapted physiology that is suited for both high growth and rapid lipid allocation at lower temperatures (Laurel et al. 2016; Copeman et al. 2016). In contrast, saffron cod have a eurythermic physiology that is better suited for survival in a warming Arctic (Laurel et al. 2016; Copeman et al. 2017). In addition to potential changes in their growth and survival due to warming, climate-mediated changes in the distribution and abundance of these species will likely have profound effects on the Arctic marine ecosystem.

The objectives of this research were to characterize the distribution and abundance of polar cod and saffron cod ELS in the Chukchi and western Beaufort seas and to better understand how these species might respond to a changing ocean environment. We expected that polar cod, a stenothermic species, would have strong responses to changing environmental conditions, particularly temperature, while saffron cod, a eurythermic species, would be less sensitive to similar environmental forcing. Findings of this study will provide important baseline information about their ELS, which can be used to identify and describe essential fish habitat (EFH) for larvae and age-0 juveniles in Alaskan waters, as required by law (U.S. Sustainable Fisheries Act 1996). Additionally, this information can be used to inform individual-based models (IBMs) developed to identify polar cod and saffron cod spawning locations and source/sink populations, and will improve our general knowledge of habitat important to their ELS, which can lead to more effective population management in a changing climate and in anticipation of increased human development in the region.

Materials and methods

Study area

The Chukchi Sea consists of a broad (~ 500 km), shallow (~ 50 m) shelf extending ~ 800 km northward from Bering Strait to the Chukchi Slope. Inflow from the northern Bering Sea is driven by the seasonally fluctuating Pacific–Arctic pressure gradient (Stigebrandt 1984; Aagaard et al. 2006), which brings freshwater, nutrients, heat, carbon, and organisms into the Chukchi Sea through Bering Strait (Wyllie-Echeverria et al. 1997; Weingartner et al. 2005; Woodgate et al. 2005; Moore and Stabeno 2015). The northward flow is comprised of cold, relatively saline, and nutrient-rich Anadyr Water (AW) in the west (Sambrotto et al. 1984); relatively warm, low-salinity Alaska Coastal Water (ACW) in the east; and Bering Shelf Water (BSW), which is a mixture of the two water masses (Coachman et al. 1975). Water travels over the Chukchi shelf along three main pathways: Herald Canyon in the west, the Central Channel across the mid-shelf, and Barrow Canyon in the east (Fig. 1). After exiting Barrow Canyon, water either flows westward along the Chukchi shelf break as the Chukchi Slope Current, or eastward into the Beaufort Sea along the shelf break and slope (Corlett and Pickart 2017). Flow over much of the shelf responds rapidly to local winds and can be highly variable, even reversing at times (Weingartner et al. 2005; Woodgate et al. 2005; Danielson et al. 2017). During the summer and fall, low-salinity waters associated with coastal run off and solar heating are transported northward by the seasonal Alaska Coastal Current (ACC, Coachman et al. 1975). During the late fall to early winter, the water column cools to near-freezing temperatures and remains near the freezing point until late spring and early summer, when increased solar radiation and the arrival of warmer water from the Bering Sea lead to rapid warming, melting of sea ice, and increased river discharge (Weingartner et al. 2005; Danielson et al. 2017).

Fig. 1 Map of the study region showing typical flow pathways of the Chukchi Sea and western Beaufort Sea based on Corlett and Pickart (2017). *BS* Bering Strait, *KS* Kotzebue Sound, *LB* Ledyard Bay

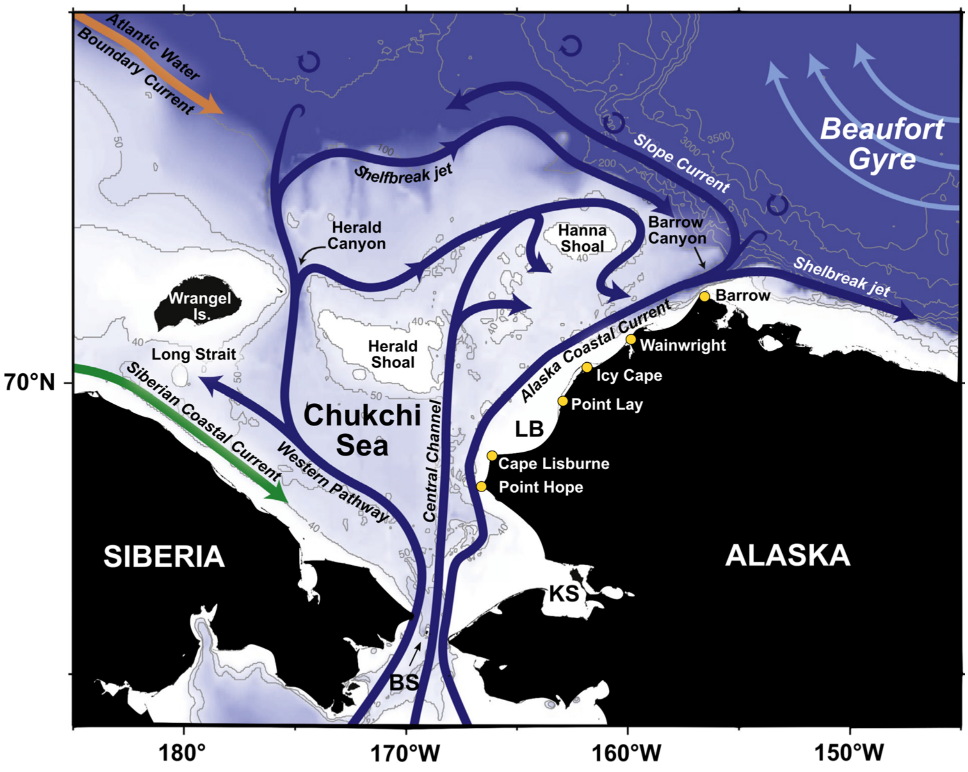

Data sources

We used data on the abundance and length composition of larval (preflexion and flexion) and juvenile polar cod and saffron cod from two primary sources: (1) ichthyoplankton surveys conducted in the Chukchi and Beaufort seas between 2004 and 2013, and (2) acoustic-trawl surveys conducted in the Chukchi Sea during 2012 and 2013 as part of the Arctic Ecosystem Integrated Survey (Arctic Eis, Mueter et al. 2017).

Ichthyoplankton surveys

To characterize the horizontal distributions of polar cod and saffron cod larvae in the northern Bering, Chukchi, and western Beaufort seas, historical larval abundance and length data, including sampling date, geographic sampling location (latitude and longitude), and bottom depth at each sampling location were obtained from the Ichthyoplankton Information System database at NOAA's Alaska Fisheries Science Center (AFSC; Table 1). Data were collected during surveys conducted by the AFSC (2004, 2005, 2008), the Russian-American Long-term Census of the Arctic (RUSALCA: 2004, 2009, 2012), and the Arctic Eis program (2012, 2013). Apart from Arctic Eis, which sampled nearly identical stations in both 2012 and 2013, these surveys varied in the geographical regions sampled but mostly occurred during August and September over the course of a decade (Table 1).

Depth-integrated ichthyoplankton samples were collected using 60-cm diameter Bongo nets (333- or 505-µm mesh) equipped with flowmeters and towed obliquely from the surface to near-bottom depths. Specimens were preserved using a buffered 5% formalin–seawater solution, after which fish larvae were transferred to 70% ethanol. Ichthyoplankton were identified to the lowest possible taxon, enumerated, and measured at the Plankton Sorting and Identification Center in Szczecin, Poland, and subsequently verified by AFSC staff using information found in Matarese et al. (1989). Catch-per-unit-effort (CPUE) for each station was calculated as the number of larvae caught under 10 m^{-2} of sea surface area. A correction factor of + 1.9% was applied to standard length (SL) records to account for shrinkage in formalin (D. Blood, B. Laurel, NOAA, unpublished data) and each measured fish was assigned to a development stage based on those described in Matarese et al. (1989) and available literature (Table 2). At present, polar cod eggs cannot be definitively distinguished from those of walleye pollock (*Gadus chalcogrammus*) (D. Blood, M. Busby, NOAA, personal communication); thus, egg data were excluded from the analysis.

Acoustic-trawl surveys

In 2012 and 2013, the Arctic Eis program conducted comprehensive ecosystem surveys of the U.S. northern Bering Sea and Chukchi Sea shelves (Mueter et al. 2017). The surveys began on 7 August and progressed northward from Bering Strait along designated transects until reaching the Chukchi shelf break by the first week of September, after which sampling recommenced in Bering Strait and progressed southward to 60 °N until the last week of September.

Acoustic-trawl (AT) methods were used to estimate the abundance and distribution of pelagic organisms during each survey. The AT surveys (see De Robertis et al. 2017a, b for details) provide the best available information about the distributions of the abundant pelagic age-0 polar cod and saffron cod present in this environment during late summer. Acoustic backscatter was measured continuously along transects on a 1.0° longitude and 0.5° latitude grid using a calibrated echosounder. Trawl samples and estimates of

Table 1 Cruise information for polar cod (*Boreogadus saida*) and saffron cod (*Eleginus gracilis*) early life stages caught in 60-cm diameter Bongo nets north of Bering Strait (≥ 65.75 °N) from the Alaska Fisheries Science Center's (AFSC) Ichthyoplankton Information System database

Survey year	Date range of samples	Survey month	Cruise/Survey name	Number of Bongo net samples	Number of samples with catch		Number of fish measured	
					Polar cod	Saffron cod	Polar cod	Saffron cod
2004	8/13–8/22	Aug.	1KR04/RUSALCA	17	8	1	101	1
2008	8/6–8/21	Aug.	1OE08	38	17	5	60	7
2009	9/6–9/29	Sep.	1KR09/RUSALCA	22	5	–	16	–
2012	8/30–9/15	Aug.–Sep.	1KR12/RUSALCA	19	1	–	50	–
	8/7–8/21	Aug.	1BE12/Arctic Eis	63	4	1	7	1
	8/27–9/10	Aug.–Sep.	2BE12/Arctic Eis	39	6	–	6	–
2013	8/7–8/17	Aug.	BE13−01/Arctic Eis	41	4	5	4	6
	8/22–9/10	Aug.–Sep.	BE13−02/Arctic Eis	58	23	–	30	–

Data were collected during surveys conducted by the AFSC, the Russian-American Long-term Census of the Arctic (RUSALCA), and the Arctic Ecosystem Integrated Survey (Arctic Eis)

Table 2 Polar cod (*Boreogadus saida*) and saffron cod (*Eleginus gracilis*) development stages and the number of samples of each stage collected north of Bering Strait (≥ 65.75 °N) using 60-cm diameter Bongo nets

Polar cod stage	Length (mm SL)	Number	Saffron cod stage	Length (mm SL)	Number
Egg	1.53–1.90 mm (diameter)	0	Egg	1.30–1.70 mm (diameter)	0
Yolksac	< 8.5	0	Yolksac	3.5–8.49	0
Preflexion	8.6–10.9	14	Preflexion	8.5–10.9	0
Flexion	11.0–16.9	119	Flexion/postflexion	11.0–23.9	7
Transformation	17.0–29.9	117	Transformation	24.0–27.0	2
Early juvenile	30.0–44.9	22	Early juvenile	27.1–46.9[a]	6
Late juvenile	45.0–65.0	2	Late juvenile	47.0[a]–65.0	0

Stages are based on Matarese et al. (1989)

[a] The mean of the minimum length of transition in the Pacific and the Arctic (Wolotira 1985) was used as the length at which saffron cod begin to transition to more demersal habitats

sound scattering properties of organisms were used to convert acoustic backscatter into estimates by species and size class (De Robertis et al. 2017a, b). A combination of surface trawls conducted at pre-determined stations, and midwater trawls conducted in areas of high backscatter were used to identify the species and size composition of sound scattering organisms. A large (122-m headrope) Cantrawl rope trawl was used for all surface and midwater trawls in 2012, while in 2013, a smaller (12-m headrope) modified-Marinovich herring trawl was used for midwater sampling (De Robertis et al. 2017a). As fishes encountered in the 2012 survey were small and likely poorly retained by the Cantrawl, a field study was conducted to determine the selectivity of the Cantrawl and modified-Marinovich trawls (De Robertis et al. 2017a). The AT abundance calculations incorporated the resulting gear, species, and size-dependent probabilities of capture (De Robertis et al. 2017b); however, the final estimates of abundance at length are sensitive to the selectivity parameters used in these calculations, particularly for the smallest size classes which are poorly retained by the trawls (De Robertis et al. 2017a, b). Abundance estimates for 10-mm size classes of polar cod and saffron cod ranging from 5 to 305 mm in length were calculated along the survey trackline. Species abundance (fish m^{-2}) at each sampling station was computed for three ELS, postflexion larvae (15–35 mm), early juveniles (35–45 mm), and late juveniles (45–65 mm), by averaging all measurements within 15 km of the nearest station.

Environmental data

Temperature and salinity data for the ichthyoplankton analysis were obtained from conductivity, temperature, and depth (CTD) measurements taken concurrently with plankton sampling at each survey station. For stations with missing CTD data (8.1% of stations), temperature and salinity data were obtained from the closest station in space and/or time. When more than one adjacent station was used, measurements were averaged (Online Resource 1).

To examine the relationship between ice and Arctic gadid ELS, the distance (in km) from each sampling station to the sea-ice edge was calculated from Multisensor Analyzed Sea Ice Extent-Northern Hemisphere (MAISE-NH) 4-km products obtained from the National Snow and Ice Data Center (NSIDC), or the U.S. National Ice Center/Naval Ice Center for 2004 and 2005 stations, and measured using ArcGIS 10.4 (ESRI 2017). Distance to land was also calculated to determine species associations with nearshore habitats. Exploratory analyses showed that temperature and distance to the ice edge were highly correlated, as were salinity and distance to land. Thus, only temperature and salinity were used to develop statistical models.

Temperature and salinity data used in the AT survey data analysis were obtained from CTD casts conducted at each sampling station. Temperature and salinity measurements taken at the surface and just above the bottom were averaged for the analysis.

Data analysis

Ichthyoplankton survey data

Polar cod larvae were present at several survey stations in the Bering Sea; however, due to the low number of samples with positive catch (< 10%), many of which were outside the period during which the majority of data were collected (August–September), we focused our analysis on larvae found north of Bering Strait (≥ 65.75 °N) to better describe their distribution and abundance in the Chukchi and western Beaufort seas. The low number of stations with positive saffron cod catch prevented a comprehensive analysis for this species beyond a description of their general size, distribution, and abundance in the region (Table 1).

Generalized additive models (GAM) with compound Poisson-gamma distributions (Tweedie distributions with index parameter $1 < p < 2$) (Tweedie 1957; Winker et al. 2014) were used to model the effects of location (latitude and longitude) and environmental covariates (Julian day, JD; bottom depth, BD; temperature, T; and salinity, S) on the abundance of polar cod and saffron cod ELS. GAMs are very well suited to model nonlinear species–environment interactions (Hastie and Tibshirani 1990) and have been used extensively in marine ecology and to model fisheries spatial data (see Guisan et al. 2002 for a general review). The Tweedie distribution, which has a point mass at zero but is otherwise continuous, is particularly useful when there is a high proportion of zeros in the data (Shono 2008) and includes both the Poisson and negative binomial models as special cases. As year differences were confounded with geographic sampling location and given the general paucity of samples in the region, data were pooled across years and separate GAMs were developed to examine spatial patterns and temporal/environmental effects. A similar approach was used to model the mean length of polar cod ELS, but with a Gaussian distribution. Bottom depth was log-transformed to reduce the leverage and influence of a few deep stations on the regression.

The response variables $x_{(\rho,\lambda)}$ were the standardized larval and juvenile polar cod abundance (number 10 m^{-2}) or mean length (in mm SL) at location ρ, λ (in degrees longitude and latitude), which were modeled as either spatial models:

$$x_{(\rho,\lambda)} = s(\rho, \lambda) + \varepsilon_{(\rho,\lambda)} \tag{1}$$

or environmental models:

$$x_{(\rho,\lambda)} = g_1(\mathrm{JD}_{(\rho,\lambda)}) + g_2(\mathrm{BD}_{(\rho,\lambda)}) + g_3(T_{(\rho,\lambda)}) + g_4(S_{(\rho,\lambda)}) + \varepsilon_{(\rho,\lambda)}, \tag{2}$$

where g_i and s are one-dimensional (1-D, Wood 2004) and two-dimensional (2-D, Wood 2003) smoothing functions, respectively, and ε is a normally distributed error term. To avoid overfitting, the degrees of freedom for smooth terms were constrained by limiting the number of knots to four for 1-D smoothers in the environmental models and 10 for 2-D smoothers in the spatial models. The best model was chosen using a backwards-stepwise elimination process, where the model term with the highest p value was removed until a model that produced the lowest Akaike Information Criterion (AIC, Akaike 1998) was found. Smooth terms in the length model were replaced with a simple linear relationship, as the estimated degrees of freedom (edf) were equal to 1.

Acoustic-trawl survey data

The location (latitude, longitude), bottom depth, and associated temperature and salinity data from CTD measurements taken at each station were used to model the abundance of the three ELS of polar cod and saffron cod within a 15-km radius. As for the ichthyoplankton data, the analysis focused on data collected north of Bering Strait (≥ 65.75 °N) and followed the same approach to model the standardized polar cod or saffron cod abundance (mean number of fish m^{-2}) of postflexion larvae, early juveniles, and late juveniles at each location. Separate models were fit for 2012 and 2013 to account for differences in the midwater trawl nets used in the AT survey.

All statistical analyses were carried out in R (R Core Team 2017) using the ‘mgcv’ library (Wood 2006). Residual diagnostics were used to assess distributional assumptions and independence. In particular, deviance residuals were mapped and their semivariance was plotted against distance between sampling points by year to test for the presence of possible spatial auto-correlation. While we found some evidence for auto-correlation, we were unable to incorporate residual auto-correlation into the model in combination with the Tweedie distribution. Therefore, some of the model results should be interpreted with caution, as confidence intervals may be wider than shown in cases where auto-correlation was present.

Results

Ichthyoplankton survey data

A total of 297 ichthyoplankton stations north of Bering Strait were used to characterize the distribution and abundance of polar cod and saffron cod ELS. Stations were sampled between 7 August and 28 September over bottom depths ranging from 15 to 440 m. Water temperatures ranged between − 1.4 and 10.8 °C, with salinities between 24.13 and 33.87. Polar cod and saffron cod were present at 68 and 12 stations, respectively.

Polar cod ELS were measured at 66 stations, with fish ranging in size from 9.2 to 47.9 mm SL (mean and standard deviation (SD) of 18.8 ± 6.8 mm SL, $n = 274$), representing preflexion to late juvenile stages. Polar cod ELS were sampled over bottom depths ranging from 24–440 m, temperatures ranging between − 1.4 and 7.5 °C, and salinities from 28.75 to 33.87. Over 89% of polar cod ELS were collected at stations north of 69 °N. Smaller larvae were found around Barrow Canyon, along the western Beaufort shelf and slope, near Wrangel Island, and on the Chukchi shelf north of 71 °N (Fig. 2a). Transformation-sized larvae, which were also found near Barrow Canyon, were more widely dispersed over the shelf, as were early juveniles.

Saffron cod ELS were collected at 12 stations, with fish ranging in size from 13.2 to 43.8 mm SL (mean and SD of 25.1 ± 9.8 mm SL, $n = 15$), representing flexion to early juvenile stages. Larvae were collected over bottom depths ranging from 15 to 114 m, temperatures between 0.2 and 8.8 °C, and salinities between 28.65 and 32.43. Flexion- and postflexion-sized larvae were found just east of Barrow Canyon, while most transformation-sized larvae and early juveniles were found farther south, below 69.5 °N (Fig. 2b). Saffron cod abundance was highest in nearshore regions, in particular south of Point Hope and east of Barrow Canyon, and was lowest in the western Chukchi Sea (Fig. 2b).

Abundance analysis

The abundance of polar cod ELS varied significantly across the study area (GAM: $F = 8.03$, edf = 7.31, $p < 0.0001$), with the highest densities in the southern and western portions of the Chukchi Sea, especially around the Chukotka Peninsula and Wrangel Island, as well as around Barrow Canyon (Fig. 3a). Environmental factors and time of sampling also had significant effects on abundance and explained a larger proportion of the deviance (40.7%) than the spatial model (31.0%) (Table 3). The AIC-best model included Julian day (GAM: $F = 10.69$, edf = 2.90, $p < 0.0001$), bottom depth (GAM: $F = 4.79$, edf = 1.74, $p = 0.0076$), temperature (GAM: $F = 14.92$, edf = 1.00, $p = 0.0001$), and salinity (GAM: $F = 5.87$, edf = 2.76, $p = 0.0022$) (Table 3). Abundance peaked around 23 August, increased nearly linearly with increasing bottom depth, decreased linearly with increasing temperature, and tended to be higher in both fresher (coastal) waters and at higher salinities (Fig. 3b–d).

Length analysis

The spatial model confirmed significant spatial variation and patchiness in size (GAM: $F = 3.38$, edf = 7.68, $p = 0.0016$) (Fig. 4a), and the environmental model suggests that these variations may be largely explained by significant increases in size with sampling date (LR: $\beta = 0.27$, $t_{63} = 3.18$, $p = 0.0023$) (Fig. 4b) and temperature (LR: $\beta = 1.29$, $t_{63} = 3.24$, $p = 0.0019$, Fig. 4c) (Table 3). The apparent growth rate estimated from the environmental model was 0.27 mm day^{-1}, which agrees well with field estimates of growth (0.28 mm day^{-1}, Bouchard and Fortier 2011) at comparable temperatures, but is higher than laboratory estimates for ELS (0.11–0.19 mm day^{-1}, Koenker et al. 2018; Laurel et al. 2017). Field-based rates often exceed laboratory estimates, as only the survivors of size-based predation are observed, thereby selecting for faster growing individuals (Bailey and Houde 1989; Litvak and Leggett 1992).

Acoustic-trawl survey data

A total of 133 and 144 stations were used in the analyses of polar cod and saffron cod ELS abundances estimated from the AT surveys in 2012 and 2013, respectively. In general, both species occupied more stations (Table 4) and were more abundant in 2013 compared to 2012 (Figs. 5, 6, 7, 8). Polar cod ELS exhibited spatial variability across the eastern Chukchi shelf in 2012 (Tables 5, 6), with higher abundances observed over the northern portions of the survey area compared to farther south (Fig. 5a, c, e). In particular, abundances were highest off the coast between Point Lay and Icy Cape, around 70.5 to 71.0 °N. Spatial patterns

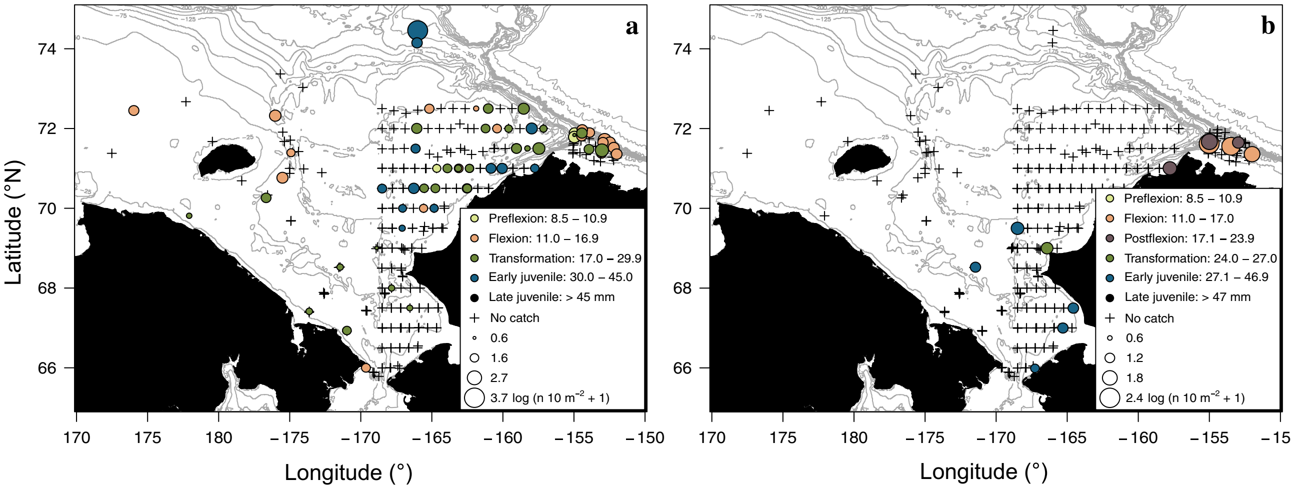

Fig. 2 Mean size (in mm SL) and log-transformed catch-per-unit-effort (n 10 m^{-2} + 1), of **a** polar cod (*Boreogadus saida*) and **b** saffron cod (*Eleginus gracilis*) early life stages collected at each sampling station using 60-cm diameter Bongo nets during surveys conducted by the Alaska Fisheries Science Center (AFSC; 2008), Russian-American Long-term Census of the Arctic (RUSALCA; 2004, 2009, 2012), and the Arctic Ecosystem Integrated Survey (Arctic Eis; 2012, 2013) in the Chukchi and western Beaufort seas

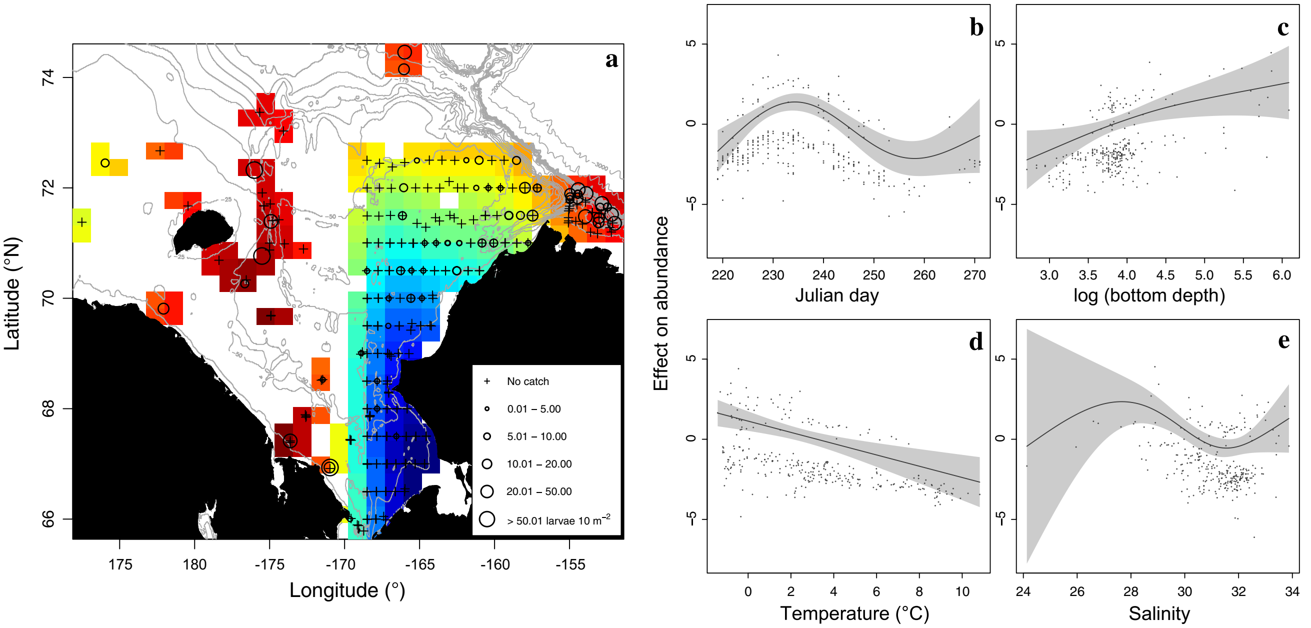

Fig. 3 Effects of location (**a**), Julian day (**b**), log-transformed bottom depth (**c**), temperature (**d**), and salinity (**e**) on the abundance of polar cod (*Boreogadus saida*) early life stages collected in the Chukchi and Beaufort seas using 60-cm Bongo nets. Spatial (**a**) and environmental (**b–e**) effects were modeled separately using generalized additive models (GAMs). For the spatial effect (**a**), darker colors represent higher abundance and lighter colors represent lower abundance. Red represents higher abundances and blue represents lower abundances in the online version. Circles are scaled to the maximum catch-per-unit-effort (176.19 larvae 10 m^{-2}). Stations with no catch are represented by (+)

Table 3 Generalized additive model (GAM) formulations for abundance and mean length (mm SL) of polar cod (*Boreogadus saida*) early life stages estimated from ichthyoplankton surveys in the Chukchi and Beaufort seas

Model	Polar cod	*n*	% dev. exp.	AIC
Abundance				
Spatial	$x_{(\rho,\lambda)} = s\ (\rho,\lambda) + \varepsilon_{(\rho,\lambda)}$	297	31.0	830.64
Environmental	$x_{(\rho,\lambda)} = g_1\ (\mathrm{JD}_{(\rho,\lambda)}) + g_2\ (\mathrm{BD}_{(\rho,\lambda)}) + g_3\ (T_{(\rho,\lambda)}) + g_4\ (S_{(\rho,\lambda)}) + \varepsilon_{(\rho,\lambda)}$	297	40.7	814.54
Length				
Spatial	$x_{(\rho,\lambda)} = s\ (\rho,\lambda) + \varepsilon_{(\rho,\lambda)}$	66	41.0	448.85
Environmental	$x_{(\rho,\lambda)} = g_1\ (\mathrm{JD}_{(\rho,\lambda)}) + g_3\ (T_{(\rho,\lambda)}) + \varepsilon_{(\rho,\lambda)}$	66	21.8	454.23

Number of observations, percent (%) deviance explained, and Akaike Information Criterion (AIC) values are shown. Length due to environmental factors was estimated using a linear model

g and *s* 1- and 2-dimensional smoothing functions, respectively, *JD* Julian day, *BD* log-transformed bottom depth, *T* temperature, *S* salinity, (ρ, λ) longitude and latitude coordinates, ε error term

accounted for 45.4 to 57.3% of the deviance, while environmental variables explained a somewhat smaller proportion of the deviance, ranging from 29.1 to 31.9% (Table 5). Polar cod abundance varied strongly with temperature, with similar responses observed across the three ELS (Fig. 5). The abundance of all stages increased with increasing temperature, reaching a peak between 5.0 and 6.0 °C, with sharp declines observed at higher temperatures (Fig. 5b, d, g). Late juvenile abundance declined with increasing bottom depth to ~ 60 m (Fig. 5f); however, depth did not significantly affect the abundance of smaller size classes (Tables 5, 6; Fig. 5).

The spatial distribution of polar cod in 2013 was similar to that in 2012, with ELS more abundant in the northern portion of the survey region compared to the south. Abundances were higher in 2013, with the highest abundances found farther south (~ 69.5–70.0 °N) and more offshore than in 2012, concentrated to the northwest of Cape Lisburne and also around Barrow Canyon (Fig. 6a, e, i). The temperature response was similar across size classes (Fig. 6c, g, k) and was similar to that found in 2012, with peak abundances between 5.0 and 6.0 °C and sharp declines at higher temperatures. However, relationships with bottom depth changed between years. While

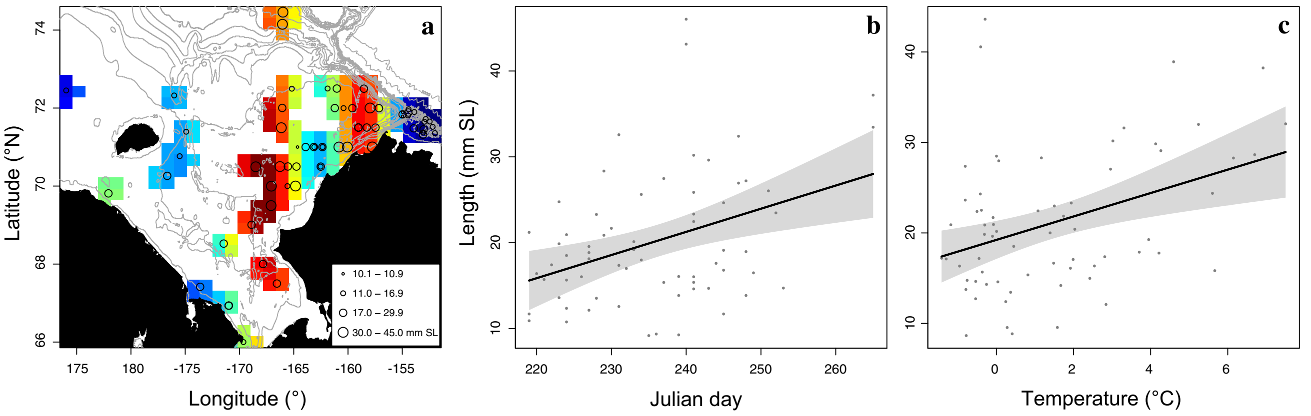

Fig. 4 Effects of location (**a**), Julian day (**b**), and temperature (**c**) on the mean length of polar cod (*Boreogadus saida*) early life stages collected in the Chukchi and Beaufort seas using 60-cm diameter Bongo nets. Spatial (**a**) and environmental (**b**, **c**) effects were modeled separately. Data for the spatial effect (**a**) were modeled using a generalized additive model (GAM) with a Tweedie distribution, which has a point mass at zero, but is otherwise continuous. A linear model with a Gaussian distribution was used to model environmental effects (**b**, **c**). For the spatial effect (**a**), darker colors represent a larger mean length and lighter colors represent a smaller mean length. Red represents a larger mean length and blue represents a smaller mean length in the online version. Circles are scaled to the maximum mean length (44.9 mm SL) of polar cod collected at each station

Table 4 Number of stations used in the acoustic-trawl survey data analysis for 2012 and 2013, along with bottom depth range (in meters), average surface–bottom temperature (mean ± SD in °C), average surface–bottom salinity (mean ± SD), and the number of stations occupied by polar cod (*Boreogadus saida*) and saffron cod (*Eleginus gracilis*) early life stages (ELS): postflexion larvae (15–35 mm), early juveniles (35–45 mm), and late juveniles (45–65 mm)

	2012	2013
Number of stations sampled (*n*)	133	144
Depth range (m)	19–99	17–101
Average surface–bottom temperature (°C)	5.17 ± 2.83	4.45 ± 3.28
Average surface–bottom salinity	30.94 ± 1.29	30.61 ± 1.28
	Number of stations occupied	
Polar cod ELS		
Postflexion larvae (15–35 mm)	39	87
Early juveniles (35–45 mm)	69	107
Late juveniles (45–65 mm)	65	92
Saffron cod ELS		
Postflexion larvae (15–35 mm)	9	33
Early juveniles (35–45 mm)	29	32
Late juveniles (45–65 mm)	37	28

bottom depth was not a significant predictor of postflexion larvae and early juveniles in 2012, it was positively associated with their abundances in 2013 (Tables 5, 6; Fig. 6b, f). Higher abundances of late juveniles were found in deeper areas in 2013 (Fig. 6j) compared to 2012 (Fig. 5f), consistent with a more offshore distribution and higher densities over Barrow Canyon. Unlike 2012, salinity was significantly associated with polar cod abundance in 2013 (Tables 5, 6). Early and late juveniles were most abundant at ~ 31.20, while the peak abundance of postflexion larvae occurred at a slightly lower salinity, ~ 30.75. Abundances of all stages declined at the highest salinities (Fig. 6d, h, l).

Spatial patterns in the abundance of saffron cod varied across ELS in 2012. High abundances of postflexion larvae were confined to a narrow region around Point Hope and Cape Lisburne (Fig. 7a). Early juveniles were also most abundant in these areas, with moderately high densities found south of Point Hope in the ACC in outer Kotzebue Sound (Fig. 7d). For both stages, a few low-density observations were found in the northeastern corner of the

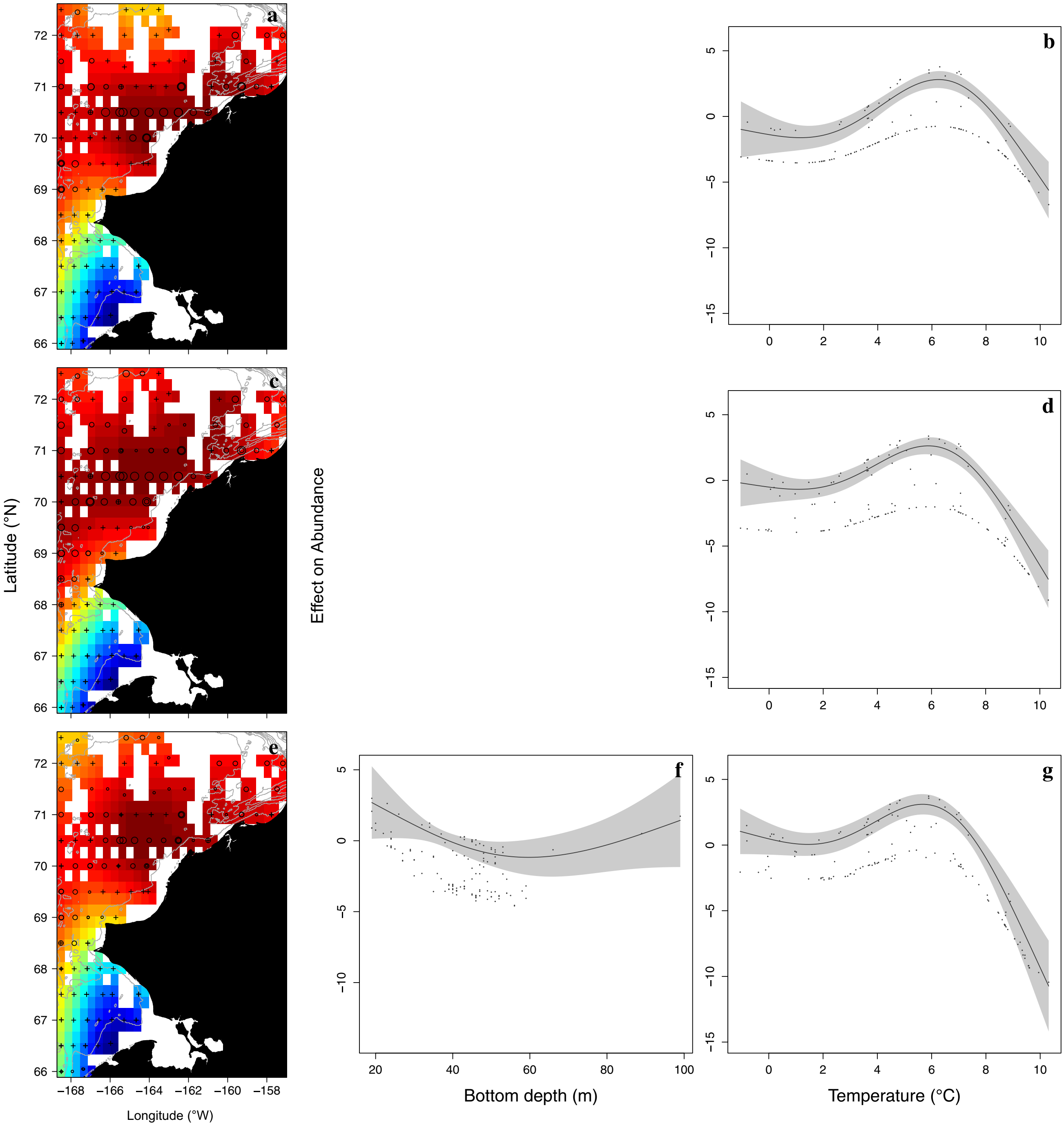

Fig. 5 From left to right, effects of location (**a**, **c**, **e**), bottom depth (**f**), temperature (**b**, **d**, **g**), and salinity (no significant effect) on the abundance of polar cod (*Boreogadus saida*) postflexion larvae (**a**, **b**), early juveniles (**c**, **d**), and late juveniles (**e**–**g**) on the Chukchi shelf estimated by the Arctic Ecosystem Integrated Survey (Arctic Eis) acoustic-trawl survey in 2012. Spatial (**a**, **c**, **e**) and environmental (**b**, **d**, **f**, **g**) effects were modeled separately using generalized additive models (GAMs). Empty panels indicate that the covariate was not included in the final model. For the spatial effect, darker colors represent higher abundances and lighter colors represent lower abundances. In the online version, red represents higher abundances and blue represents lower abundances. Circles reflect log-transformed abundances (fish m^{-2}) of 0.001, 0.1, 0.5, and greater than 0.5, to a maximum of 1.635 (postflexion larvae), 2.616 (early juveniles), and 0.139 (late juveniles). Stations where estimated abundance was zero are represented by (+)

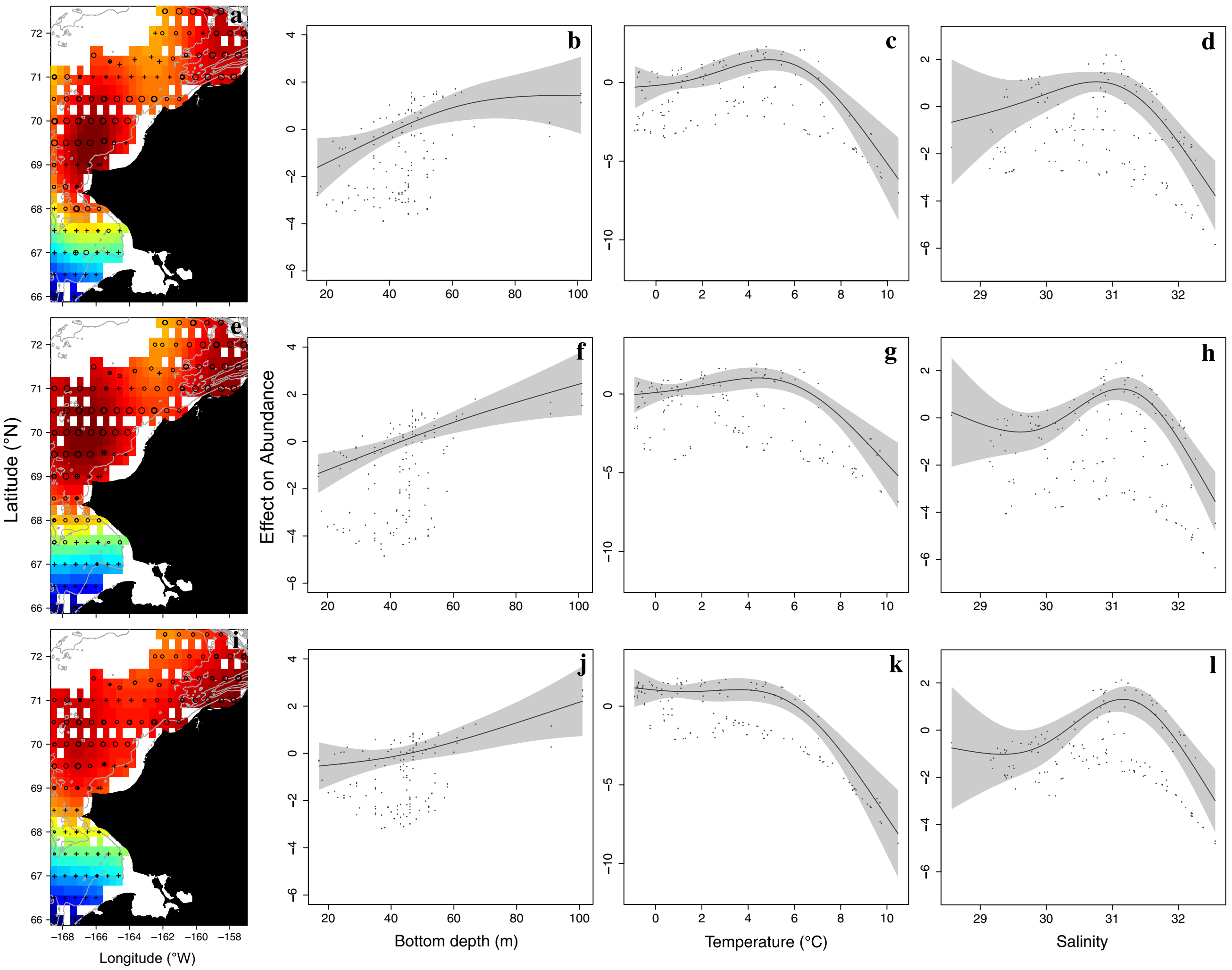

Fig. 6 From left to right, effects of location (**a**, **e**, **i**), bottom depth (**b**, **f**, **j**), temperature (**c**, **g**, **k**), and salinity (**d**, **h**, **l**) on the abundance of polar cod (*Boreogadus saida*) postflexion larvae (**a**–**d**), early juveniles (**e**–**h**), and late juveniles (**i**–**l**) on the Chukchi Sea shelf estimated by the Arctic Ecosystem Integrated Survey (Arctic Eis) acoustic-trawl survey in 2013. Spatial (**a**, **e**, **i**) and environmental (**b**–**d**, **f**–**h**, **j**–**l**) effects were modeled separately using generalized additive models (GAMs). Empty panels indicate that the covariate was not included in the final model. For the spatial effect, darker colors represent higher abundances and lighter colors represent lower abundances. In the online version, red represents higher abundances and blue represents lower abundances. Circles reflect log-transformed abundances (fish m^{-2}) of 0.001, 0.1, 0.5, and greater than 0.5, to a maximum of 2.722 (postflexion larvae), 2.562 (early juveniles), and 0.879 (late juveniles). Stations where estimated abundance was zero are represented by (+)

study area, including the Barrow Canyon region (Fig. 7a, d). Late juveniles were abundant in much of the ACC, but also extended offshore north of Cape Lisburne (Fig. 7g). Environmental covariates significantly affected the abundance of saffron cod ELS (Tables 5, 6), accounting for much of the deviance at the postflexion stage (80.6%), but a smaller proportion at the early juvenile (60.9%) and late juvenile stages (58.4%; Table 5). Abundances of all saffron cod ELS tended to increase with both bottom depth and temperature (Fig. 7), but the salinity effect was not significant (Tables 5, 6).

Spatial patterns in saffron cod abundance remained fairly consistent across the postflexion larval and early juvenile stages in 2013, with the highest abundances seen close to shore near Icy Cape south to Kotzebue Sound, and the lowest abundances found around Barrow Canyon (Fig. 8a, c). In contrast, late juvenile abundance was very low east of Icy Cape, but was high almost everywhere else (Fig. 8e). Spatial and environmental models accounted for a relatively high proportion of deviance across all stages (48.3–84.2%), except for the postflexion environmental model (26.0%) (Table 5). Temperature had

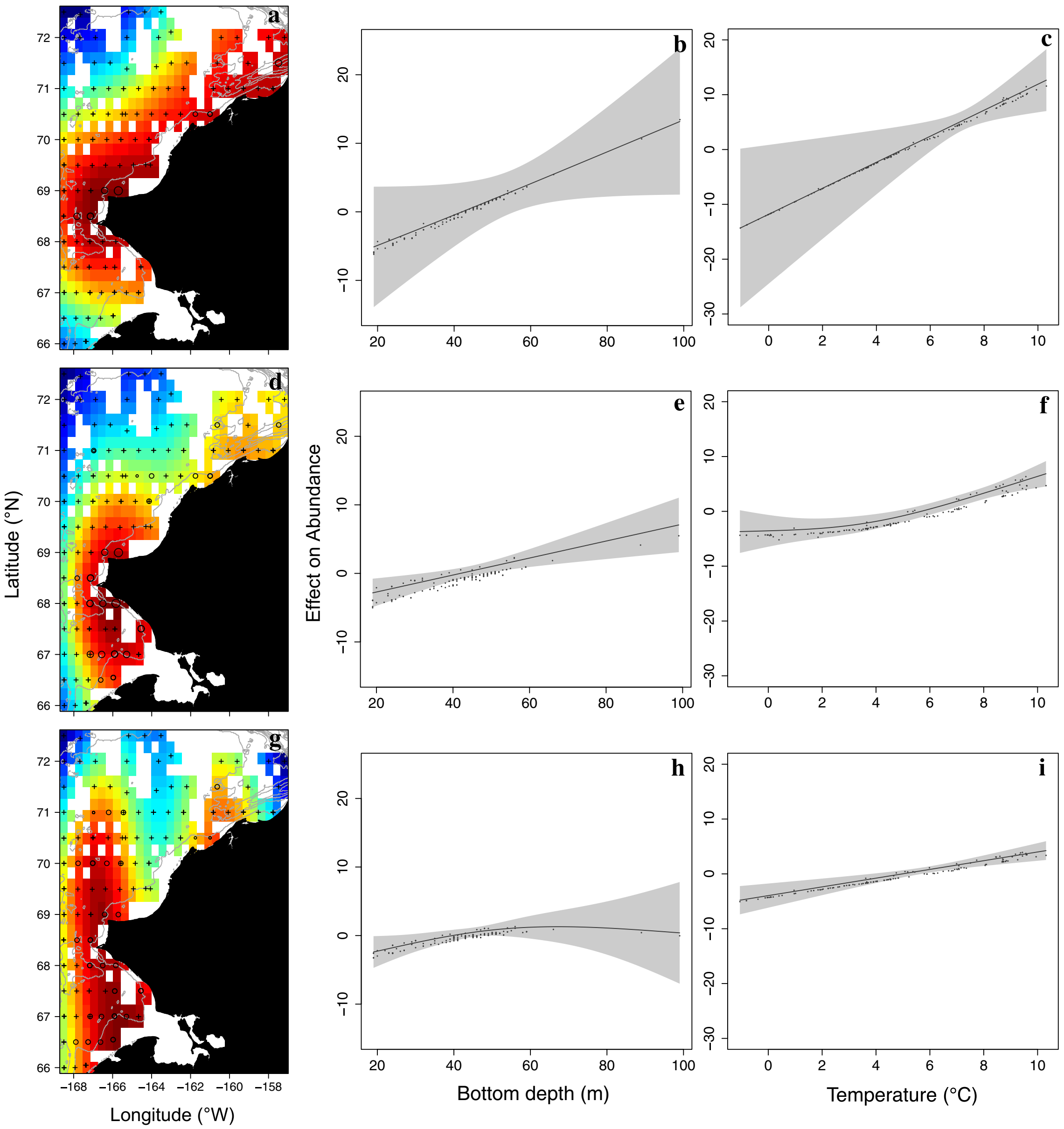

Fig. 7 From left to right, effects of location (**a**, **d**, **g**), bottom depth (**b**, **e**, **h**), temperature (**c**, **f**, **i**), and salinity (no significant effect) on the abundance of saffron cod (*Eleginus gracilis*) postflexion larvae (**a**–**c**), early juveniles (**d**–**f**), and late juveniles (**g**–**i**) on the Chukchi shelf estimated by the Arctic Ecosystem Integrated Survey (Arctic Eis) acoustic-trawl survey in 2012. Spatial (**a**, **d**, **g**) and environmental (**b**, **c**, **e**, **f**, **h**, **l**) effects were modeled separately using generalized additive models (GAMs). Empty panels indicate that the covariate was not included in the final model. For the spatial effect, darker colors represent higher abundances and lighter colors represent lower abundances. In the online version, red represents higher abundances and blue represents lower abundances. Circles reflect log-transformed abundances (fish m^{-2}) of 0.001, 0.1, 0.5, and greater than 0.5, to a maximum of 0.153 (postflexion larvae), 0.122 (early juveniles), and 0.009 (late juveniles). Stations where estimated abundance was zero are represented by (+)

a positive effect on abundance across all stages (Fig. 8b, d, g), with a notable, sharp increase with increasing temperature to ~ 4.0 °C for late juveniles. Bottom depth had a significant, positive effect on the abundance of late juveniles only (Fig. 8f). As in 2012, the salinity effect was not significant (Tables 5, 6).

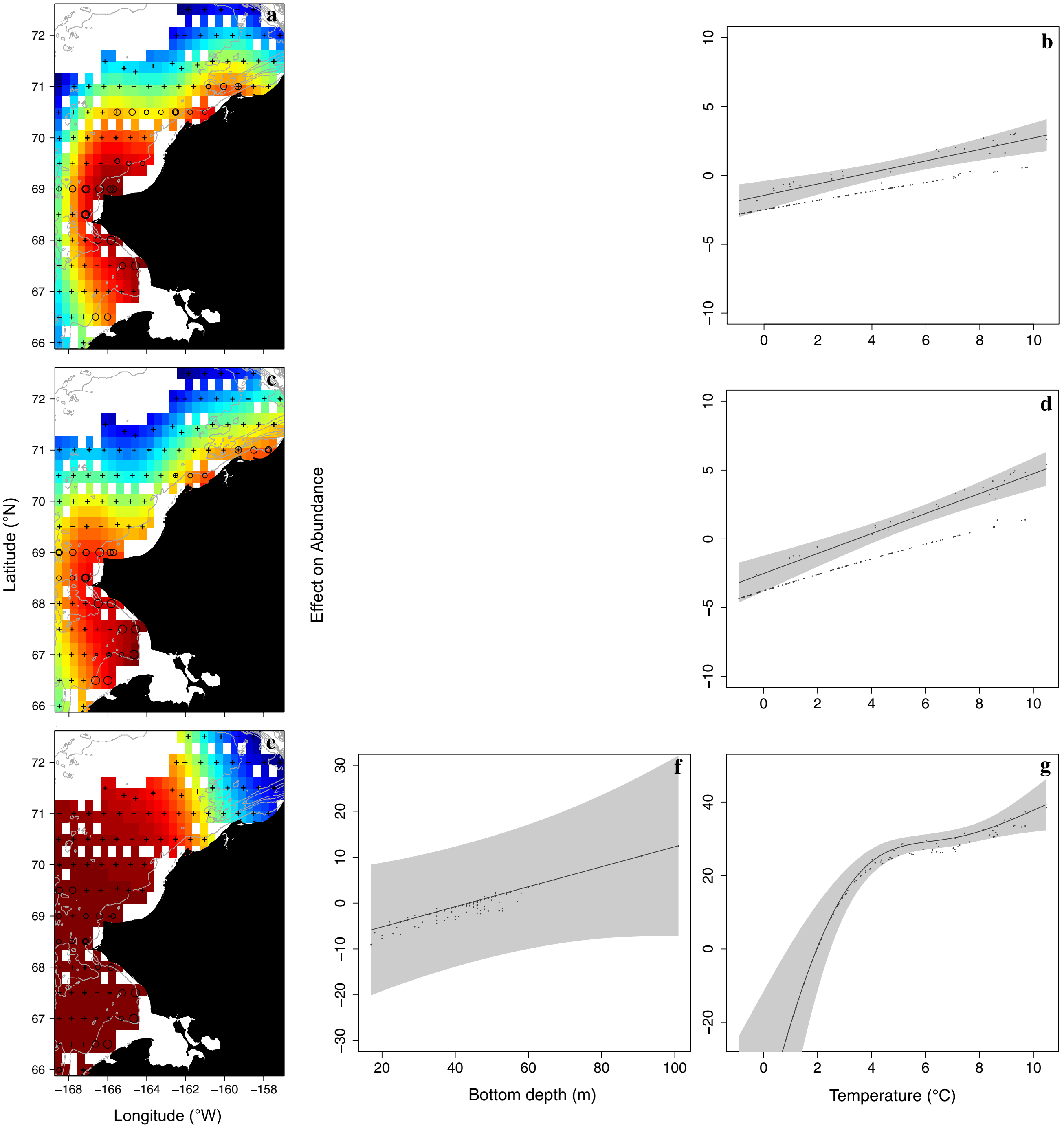

Fig. 8 From left to right, effects of location (**a**, **c**, **e**), bottom depth (**f**), temperature (**b**, **d**, **g**), and salinity (no significant effect) on the abundance of saffron cod (*Eleginus gracilis*) postflexion larvae (**a**, **b**), early juveniles (**c**, **d**), and late juveniles (**e**–**g**) on the Chukchi shelf estimated by the Arctic Ecosystem Integrated Survey (Arctic Eis) acoustic-trawl survey in 2013. Spatial (**a**, **c**, **e**) and environmental (**b**, **d**, **f**, **g**) effects were modeled separately using generalized additive models (GAMs). Empty panels indicate that the covariate was not included in the final model. For the spatial effect, darker colors represent higher abundances and lighter colors represent lower abundances. In the online version, red represents higher abundances and blue represents lower abundances. Circles reflect log-transformed abundances (fish m^{-2}) of 0.001, 0.1, 0.5, and greater than 0.5, to a maximum of 0.374 (postflexion larvae), 0.449 (early juveniles), and 0.482 (late juveniles). Note that the confidence intervals for the environmental effects extend beyond the figure at larger values and that the scale differs on the *y*-axis for the temperature effect. Stations where estimated abundance was zero are represented by (+)

Table 5 Generalized additive model (GAM) formulations for polar cod (*Boreogadus saida*) and saffron cod (*Eleginus gracilis*) abundance (fish m^{-2}) of postflexion larvae (15–35 mm), early juveniles (35–45 mm), and late juveniles (45–65 mm) estimated by the 2012 and 2013 Arctic Ecosystem Integrated Survey (Arctic Eis) acoustic-trawl surveys in the Chukchi Sea

Model	Polar cod	*n*	% dev. exp.	AIC
Spatial	2012			
Postflexion	$x_{(\rho,\lambda)} = s\,(\rho,\lambda) + \varepsilon_{(\rho,\lambda)}$	133	57.3	156.10
Early juvenile	$x_{(\rho,\lambda)} = s\,(\rho,\lambda) + \varepsilon_{(\rho,\lambda)}$	133	50.9	14.87
Late juvenile	$x_{(\rho,\lambda)} = s\,(\rho,\lambda) + \varepsilon_{(\rho,\lambda)}$	133	45.4	− 380.31
Environmental	2012			
Postflexion	$x_{(\rho,\lambda)} = g_2\,(T_{(\rho,\lambda)}) + \varepsilon_{(\rho,\lambda)}$	133	31.9	176.81
Early juvenile	$x_{(\rho,\lambda)} = g_2\,(T_{(\rho,\lambda)}) + \varepsilon_{(\rho,\lambda)}$	133	29.1	48.50
Late juvenile	$x_{(\rho,\lambda)} = g_1\,(\mathrm{BD}_{(\rho,\lambda)}) + g_2\,(T_{(\rho,\lambda)}) + \varepsilon_{(\rho,\lambda)}$	133	30.2	− 357.92
Spatial	2013			
Postflexion	$x_{(\rho,\lambda)} = s\,(\rho,\lambda) + \varepsilon_{(\rho,\lambda)}$	144	37.4	326.99
Early juvenile	$x_{(\rho,\lambda)} = s\,(\rho,\lambda) + \varepsilon_{(\rho,\lambda)}$	144	48.9	182.16
Late juvenile	$x_{(\rho,\lambda)} = s\,(\rho,\lambda) + \varepsilon_{(\rho,\lambda)}$	144	48.8	− 134.71
Environmental	2013			
Postflexion	$x_{(\rho,\lambda)} = g_1\,(\mathrm{BD}_{(\rho,\lambda)}) + g_2\,(T_{(\rho,\lambda)}) + g_3\,(S_{(\rho,\lambda)}) + \varepsilon_{(\rho,\lambda)}$	144	34.1	333.54
Early juvenile	$x_{(\rho,\lambda)} = g_1\,(\mathrm{BD}_{(\rho,\lambda)}) + g_2\,(T_{(\rho,\lambda)}) + g_3\,(S_{(\rho,\lambda)}) + \varepsilon_{(\rho,\lambda)}$	144	36.3	217.96
Late juvenile	$x_{(\rho,\lambda)} = g_1\,(\mathrm{BD}_{(\rho,\lambda)}) + g_2\,(T_{(\rho,\lambda)}) + g_3\,(S_{(\rho,\lambda)}) + \varepsilon_{(\rho,\lambda)}$	144	33.2	− 95.63
Model	Saffron cod	*n*	% dev. exp.	AIC
Spatial	2012			
Postflexion	$x_{(\rho,\lambda)} = s\,(\rho,\lambda) + \varepsilon_{(\rho,\lambda)}$	133	80.6	99.41
Early juvenile	$x_{(\rho,\lambda)} = s\,(\rho,\lambda) + \varepsilon_{(\rho,\lambda)}$	133	60.9	− 43.84
Late juvenile	$x_{(\rho,\lambda)} = s\,(\rho,\lambda) + \varepsilon_{(\rho,\lambda)}$	133	58.4	− 245.24
Environmental	2012			
Postflexion	$x_{(\rho,\lambda)} = g_1\,(\mathrm{BD}_{(\rho,\lambda)}) + g_2\,(T_{(\rho,\lambda)}) + \varepsilon_{(\rho,\lambda)}$	133	56.7	95.51
Early juvenile	$x_{(\rho,\lambda)} = g_1\,(\mathrm{BD}_{(\rho,\lambda)}) + g_2\,(T_{(\rho,\lambda)}) + \varepsilon_{(\rho,\lambda)}$	133	40.0	− 32.41
Late juvenile	$x_{(\rho,\lambda)} = g_1\,(\mathrm{BD}_{(\rho,\lambda)}) + g_2\,(T_{(\rho,\lambda)}) + \varepsilon_{(\rho,\lambda)}$	133	27.8	− 220.18
Spatial	2013			
Postflexion	$x_{(\rho,\lambda)} = s\,(\rho,\lambda) + \varepsilon_{(\rho,\lambda)}$	144	52.1	25.12
Early juvenile	$x_{(\rho,\lambda)} = s\,(\rho,\lambda) + \varepsilon_{(\rho,\lambda)}$	144	66.9	26.79
Late juvenile	$x_{(\rho,\lambda)} = s\,(\rho,\lambda) + \varepsilon_{(\rho,\lambda)}$	144	84.2	− 47.24
Environmental	2013			
Postflexion	$x_{(\rho,\lambda)} = g_2\,(T_{(\rho,\lambda)}) + \varepsilon_{(\rho,\lambda)}$	144	26.0	35.75
Early juvenile	$x_{(\rho,\lambda)} = g_2\,(T_{(\rho,\lambda)}) + \varepsilon_{(\rho,\lambda)}$	144	48.3	35.07
Late juvenile	$x_{(\rho,\lambda)} = g_1\,(\mathrm{BD}_{(\rho,\lambda)}) + g_2\,(T_{(\rho,\lambda)}) + \varepsilon_{(\rho,\lambda)}$	144	75.7	− 39.28

Number of observations, percent (%) deviance explained, and Akaike Information Criterion (AIC) values are shown. Terms in gray were not significant, but remained in the model, as their inclusion produced the lowest AIC value

g and *s* 1- and 2-dimensional smoothing functions, respectively, *BD* bottom depth, *T* average surface–bottom temperature, *S* average surface–bottom salinity, (ρ, λ) longitude and latitude coordinates, ε error term

Discussion

Differences in the distributions of polar cod and saffron cod suggest habitat partitioning at the larval and juvenile stages. However, their distributions overlapped in some areas, particularly near Barrow Canyon, where larvae of both species were abundant in Bongo net samples. While the AT survey detected high abundances of polar cod ELS in both 2012 and 2013 over most of the northern Chukchi shelf, especially from Cape Lisburne to Icy Cape, these were areas of particularly low abundance in the ichthyoplankton survey data. The highest abundances of early stages of polar cod estimated by the ichthyoplankton spatial model were found outside of the Arctic Eis survey area, specifically, around Barrow Canyon, in the western Beaufort Sea, along the Chukotka Peninsula, and around

Table 6 Generalized additive model (GAM) results for spatial and environmental models developed for polar cod (*Boreogadus saida*) and saffron cod (*Eleginus gracilis*) postflexion larvae (15–35 mm), early juveniles (35–45 mm), and late juveniles (45–65 mm) based on abundances estimated by the 2012 and 2013 Arctic Ecosystem Integrated Survey (Arctic Eis) acoustic-trawl surveys in the Chukchi Sea

Model	Postflexion larvae			Early juveniles			Late juveniles		
	F	edf	p value	F	edf	p value	F	edf	p value
Polar cod									
2012									
Spatial									
$s\ (\rho,\lambda)$	7.53	8.49	< 0.0001	14.12	8.64	< 0.0001	20.46	8.39	< 0.0001
Environmental									
$g_1\ (\mathrm{BD}_{(\rho,\lambda)})$	–	–	–	–	–	–	2.46	2.23	0.0557
$g_2\ (T_{(\rho,\lambda)})$	22.49	2.90	< 0.0001	23.91	2.93	< 0.0001	20.43	2.93	< 0.0001
$g_3\ (S_{(\rho,\lambda)})$	–	–	–	–	–	–	–	–	–
2013									
Spatial									
$s\ (\rho,\lambda)$	8.20	8.22	< 0.0001	18.17	8.43	< 0.0001	17.73	8.36	< 0.0001
Environmental									
$g_1\ (\mathrm{BD}_{(\rho,\lambda)})$	5.77	1.84	0.0027	10.84	1.28	0.0002	5.78	1.55	0.0106
$g_2\ (T_{(\rho,\lambda)})$	7.70	2.78	< 0.0001	8.07	2.71	< 0.0001	17.47	2.72	< 0.0001
$g_3\ (S_{(\rho,\lambda)})$	13.32	2.66	< 0.0001	16.59	2.87	< 0.0001	13.38	2.83	< 0.0001
Saffron cod									
2012									
Spatial									
$s\ (\rho,\lambda)$	2.88	8.04	0.0041	16.71	7.65	< 0.0001	10.47	8.32	< 0.0001
Environmental									
$g_1\ (\mathrm{BD}_{(\rho,\lambda)})$	3.62	1.10	0.0653	11.59	1.00	0.0009	2.26	2.20	0.0904
$g_2\ (T_{(\rho,\lambda)})$	7.49	1.00	0.0071	12.89	2.26	< 0.0001	19.19	1.00	< 0.0001
$g_3\ (S_{(\rho,\lambda)})$	–	–	–	–	–	–	–	–	–
2013									
Spatial									
$s\ (\rho,\lambda)$	9.05	7.93	< 0.0001	12.22	8.21	< 0.0001	209.90	8.98	< 0.0001
Environmental									
$g_1\ (\mathrm{BD}_{(\rho,\lambda)})$	–	–	–	–	–	–	9.38	1.00	0.0026
$g_2\ (T_{(\rho,\lambda)})$	21.89	1.00	< 0.0001	49.77	1.00	< 0.0001	19.64	1.00	< 0.0001
$g_3\ (S_{(\rho,\lambda)})$	–	–	–	–	–	–	1.91	2.56	0.1446

F statistics, estimated degrees of freedom (edf), and p values are shown

g and s 1- and 2-dimensional smoothing functions, respectively, *BD* bottom depth, T average surface–bottom temperature, S average surface–bottom salinity (ρ, λ) longitude and latitude coordinates

Wrangel Island, which suggests that the large numbers of older juveniles observed in the AT survey area may have been transported there from elsewhere. This is consistent with the observation of high abundances of young-of-the-year polar cod in this area, but relatively few adults in AT and bottom trawl surveys (De Robertis et al. 2017b). Higher densities of polar cod ELS found over the western portion of the Chukchi shelf suggest that the western Chukchi Sea may support greater abundances of juvenile polar cod in general (Nikolayev et al. 2008). Indeed, a 2017 AT survey in the Arctic Eis sampling region found that juvenile polar cod were most abundant in the northwest portion of the survey area, with higher abundances than those observed in previous years (A. De Robertis, unpublished data). Although only a few stations were sampled over the Chukchi slope and Arctic Basin during the ichthyoplankton surveys, those samples yielded high densities of polar cod, particularly early juveniles. A recent ichthyoplankton survey conducted in late summer 2017 also encountered polar cod ELS over the slope, although these fish appeared to be smaller in size (M. Busby, NOAA, personal communication). While the origin of these fish is unknown, the slope habitat may be important for polar cod ELS, as well as for age-1 + polar cod (e.g., Parker-Stetter et al. 2011).

Depth, temperature, and salinity are three important abiotic habitat features influencing the distribution of marine fishes (Laprise and Pepin 1995; Abookire et al. 2000). These factors, particularly temperature, were important in structuring the distribution and abundance of polar cod and saffron cod ELS in the Chukchi and Beaufort seas. However, habitat associations varied between the two species, between years and, to a lesser extent, between ELS. Within the Arctic Eis survey area, we found that polar cod were distributed farther north (> 69 °N) and more offshore than saffron cod, which were predominantly found south of 70.5 °N and closer to shore. Our results agree well with what is generally known about the distributions of the two species in Alaska's Arctic (Wolotira 1985; Mecklenburg et al. 2002; Logerwell et al. 2015; De Robertis et al. 2017b). These distributional differences effectively result in habitat partitioning of the Chukchi shelf, most likely due to species-specific thermal and salinity tolerances, as well as advective processes. Indeed, currents and water column temperatures and salinities are known to structure ichthyoplankton habitats in the Chukchi Sea (Norcross et al. 2010). Wyllie-Echeverria et al. (1997) noted that changes in the distribution and abundance of age-0 polar cod coincided with the boundary between Resident Chukchi Water (or Winter Water, WW) and ACW, where a semi-permanent front forms along the bottom between 70 and 71 °N (Weingartner 1997). High concentrations of age-0 fish were associated with low temperature (< 1 °C) and high salinity (32–33) WW. In contrast, De Robertis et al. (2017b) and this study found that age-0 polar cod were abundant at intermediate temperatures and high salinities in areas of the northern Chukchi shelf influenced by the Bering-Chukchi Summer Water (BCSW). Saffron cod were abundant at higher temperatures and lower salinities associated with ACW over relatively shallow water (< 50 m). This is consistent with other studies that have found age-0 saffron cod in nearshore habitats, mostly occurring at depths less than 40 m (Wolotira 1985; Logerwell et al. 2015; De Robertis et al. 2017b).

Both species exhibited habitat associations that may reflect interannual differences in circulation. Polar cod ELS were most abundant in shallower parts of the Arctic Eis survey area in 2012 and in deeper parts in 2013. In contrast, saffron cod were more abundant at deeper depths in 2012 and 2013, but associations were weak or not significant. Weak and variable associations with water depth contrast with a relatively strong and consistent temperature association between years, and likely reflect associations with specific water masses, combined with interannual changes in the dominant circulation patterns that redistribute water masses across the shelf. The moderate amount of deviance explained by environmental covariates in most cases and differences in the apparent effects between years suggest that other factors are important in determining the abundance and distribution of polar cod and saffron cod ELS. In particular, we expect the distribution of larval stages to be driven by advective processes, which can be highly variable among years (Danielson et al. 2017).

Contrasting responses to temperature were identified in the abundance and length models developed for polar cod ELS based on ichthyoplankton survey data, with abundance declining and length increasing at higher temperatures. Sharp declines in AT survey abundances were also associated with higher temperatures, with similar responses found among all three polar cod ELS. Similar temperature responses across ELS can likely be attributed to the fact that polar cod is a cold-water, stenothermic species with a narrow thermal window (Laurel et al. 2016, 2017). De Robertis et al. (2017b), using the same AT survey data, found that age-0 polar cod were abundant at intermediate temperatures (3.4–6.6 °C in 2012 and 2.6–6.7 °C in 2013) in areas of the northern Chukchi shelf influenced by the BCSW. In the current study, peak abundances of all three polar cod size classes occurred between 5.0 and 6.0 °C in both years, which is similar to the temperatures of maximum growth ($T_{\max}$) determined from laboratory experiments for first-feeding and preflexion larvae ($T_{\max =}$ 5.2 °C and 6.7 °C, respectively, Koenker et al. 2018) and juveniles ($T_{\max =}$ 6.4 °C, Laurel et al. 2017). Sharp declines in survey abundances at higher temperatures are consistent with the findings of Koenker et al. (2018), where notable declines in laboratory survival of polar cod preflexion feeding stages occurred at temperatures above 5 °C. At temperatures below this threshold, survival and early growth of polar cod have been positively correlated with warmer sea surface temperatures (Fortier et al. 2006; Bouchard and Fortier 2008, 2011). A progressively earlier ice breakup may initially improve the recruitment of juvenile polar cod in the fall by increasing growth and survival of early hatchers, however, increasingly earlier ice breakups will eventually become detrimental to their survival once thermal tolerances are exceeded (Bouchard et al. 2017). Further warming may also impact ice algae production, affecting copepod reproduction and the abundance of their nauplii, which are primary prey of first-feeding polar cod (Bouchard et al. 2017). This may be particularly relevant to polar cod, as they are more prone to starvation with warming than related gadids (Laurel et al. 2016).

Temperature associations were fairly similar across all three saffron cod ELS, with abundance increasing linearly with increasing temperature and higher abundances above 4.0–6.0 °C. Few studies have examined the temperature responses of larval and juvenile saffron cod, but recent work has shown that saffron cod larvae < 10 mm in length are stenothermic, tolerating a narrow range of temperatures, in contrast to older early juvenile stages, which tolerate a broader range of temperatures (B. Laurel, NOAA, personal communication; Laurel et al. 2016).

Polar cod exhibited variable associations with salinity across ELS in 2013, but responses in 2012 were not significant. Peak hatching of polar cod eggs occurs in May and June, which coincides with the timing of ice break up (Borkin et al. 1986; Bouchard and Fortier 2008), though hatching occurs as late as July in the Chukchi Sea and other Arctic regions (Wyllie-Echeverria et al. 1997; Bouchard and Fortier 2011). Newly hatched polar cod larvae are able to survive widely fluctuating salinities after ice melt (Sakurai et al. 1998). Variable associations between salinity and ELS are expected, as sea-ice melt and river discharges in summer can significantly alter the salinity signature of water masses on the Chukchi shelf (Danielson et al. 2017). However, age-0 polar cod in the Barents Sea preferred salinities between 33.7 and 34.8, and occupied more saline waters within the preferred salinity range in warmer years compared to colder ones (Rajasakaren 2013). Combined, these findings suggest that polar cod ELS are euryhaline, tolerating a wide range of salinities encountered in the highly variable and seasonal Arctic ecosystem. Associations between saffron cod abundance and salinity were not significant, which suggests that their ELS may also tolerate a wide range of salinities. Recent laboratory work has shown that larvae of both species are highly tolerant to salinity fluctuations (M. Spencer, NOAA, unpublished data). Salinity preferences for saffron cod are known to change by season and are associated with developmental changes, as well as with spawning and feeding behavior (Nikolski 1954; Wolotira 1985).

Observed relationships between polar cod and saffron cod ELS and temperature and salinity likely reflect the two species' associations with particular water masses. Water mass properties on the Chukchi shelf differed considerably between 2012 and 2013 (Danielson et al. 2017). Near-bottom BCSW was more saline in 2012 and ACW was warmer in 2013, but did not extend as far north due to persistent winds from the northeast that that led to flow reversals over much of the northeast Chukchi Sea and limited the northward extent of the ACC. As a result, cooler Melt Water covered a larger portion of the northeast Chukchi shelf in 2013, extending all the way to the northwest Alaskan coast, where ACW is normally found (Danielson et al. 2017). Changes in the temperature and salinity responses of polar cod and saffron cod ELS between 2012 and 2013 likely result from wind-induced changes in the distribution of water masses. In the Beaufort Sea, polar cod are known to change their distribution based on daily movements of the shoreward edge of the marine water mass (Moulton and Tarbox 1987), and different current regimes can affect the distribution and abundance of saffron cod in the Sea of Japan (Vasil'kov et al. 1981).

In the AT survey data analysis, surface and bottom temperatures and salinities from CTD casts were averaged to reflect the environmental properties of the water column over which acoustic measurements were taken. While surface and bottom temperatures are highly correlated, they diverge in strongly stratified areas, for example, where ACW overlays BCSW (Danielson et al. 2017; Marsh et al. 2017). As the vertical distribution of ELS was not resolved, associating a particular stage with a specific water mass was not possible, which limits the ability to determine more precise relationships with environmental variables at this time. Complicating matters further is that different populations of polar cod and saffron cod may exist in the region, and may show population-specific responses to environmental variables. Based on growth data in the Kara, Laptev, and Barents seas, two forms of polar cod exist: a slow-growing form found in coastal regions of the Kara and Laptev seas and a fast-growing form associated with marine waters of the Barents and Kara seas (Moskalenko 1964). Differences between the two forms have also been noted in juvenile polar cod (N. Chernova, Zoological Institute of Russian Academy of Sciences, personal communication). In the northern Bering and Chukchi seas, Helser et al. (2017) found regional differences in growth for both polar cod and saffron cod, but it is not known if regional differences in growth exist for their ELS in the Chukchi Sea.

Abundance estimates of age-0 polar cod and saffron cod from the AT survey were 3–4 times higher for both species in 2013 compared to 2012 (De Robertis et al. 2017b; Figs. 5, 6, 7, 8). Despite substantial differences in wind forcing and circulation over the Chukchi shelf (Danielson et al. 2017), their spatial distributions remained relatively consistent between years, which suggests that their large-scale summer distributions over the survey area are relatively insensitive to variability in environmental forcing. Indeed, species have likely adapted over time to maximize their dispersal success, reducing losses from advection by spawning in areas where local bathymetric features and prevailing currents deliver their larvae to appropriate nursery grounds (Iles and Sinclair 1982; Bailey and Picquelle 2002; Bailey et al. 2008; Duffy-Anderson et al. 2014). As a result, distribution patterns are expected to remain relatively consistent between years. However, drift pathways may be altered by deviations from average conditions (Bailey et al. 2005). Despite general similarities between the 2012 and 2013 Arctic Eis surveys, a southward shift in the distributions of both species was evident, most notably, increased presence in 2013 of age-0 polar cod south of Point Hope and decreased presence of saffron cod around Barrow Canyon compared to 2012. From late December 2012 to March 2013, nearly continuous upcanyon flow was recorded at Mooring BC2 at the head of

Barrow Canyon, while essentially no net flow was recorded along the canyon axis over a similar time period in 2012 (January–April; Danielson et al. 2017). Southward shifts in distribution in 2013 may result from increased up-canyon flows during the spawning and hatching season, resulting in more southwestward transport of polar cod eggs and larvae onto the Chukchi shelf from adult populations in the Beaufort Sea (Geoffroy et al. 2011; Parker-Stetter et al. 2011; Benoit et al. 2014). Winds in August 2013 were also more directionally polarized than those in 2012, blowing toward the south and southwest for nearly half the month, shutting down a portion of the ACC, and likely promoting upwelling in Barrow Canyon for several weeks (Danielson et al. 2017). During this time, polar cod and saffron cod larvae in the northern portion of the survey area were likely transported southward, with reduced northeast transport in the ACC leading to increased retention of larvae in the southern portion of the survey area in 2013.

During winter 2012/2013, an extensive coastal polynya developed from Point Barrow to south of Point Hope, which was associated with the flow reversal in Barrow Canyon (Danielson et al. 2017). Higher abundances of both polar cod and saffron cod in 2013 could potentially be associated with this open water feature, as the upwelling of deep (200 m), warm water (> − 1 °C) Atlantic Water from the Arctic Basin onto the Chukchi shelf through Barrow Canyon (Ladd et al. 2016) may have provided eggs and larvae with an important thermal refuge from near-freezing shelf temperatures during winter, reducing egg development times and larval stage duration. Polynyas are also thought to provide the light necessary for first-feeding larvae to detect and capture plankton prey (Bouchard and Fortier 2008), which can lead to increased survival during this critical stage. Faster growth and larger size-at-age associated with frequent winter–spring polynyas and longer open water periods may be advantageous to larvae (Fortier et al. 2006; Bouchard and Fortier 2008), not only through their improved ability to capture prey and avoid predation in the surface layers ("bigger is better hypothesis", Miller et al. 1988), but also by reaching a larger size before migrating to depth in the fall, thus limiting cannibalism (Bouchard and Fortier 2011) and increasing overwinter survival, which is known to be an important mechanism controlling the recruitment of walleye pollock in the Bering Sea (Heintz et al. 2013).

Of particular interest is that small polar cod and saffron cod larvae were encountered in both the ichthyoplankton and AT surveys in the northern part of the Chukchi Sea, particularly around Barrow Canyon. Spawning may have occurred farther south, with eggs and larvae subsequently transported by the ACC and other shelf currents into Barrow Canyon and onto the western Beaufort shelf. Alternatively, spawning may have taken place in close proximity to Barrow Canyon and larvae were retained in the area. Polar cod and saffron cod are thought to spawn and develop on the Beaufort shelf (Craig and Haldorson 1981; Craig et al. 1982; Parker-Stetter et al. 2011; Benoit et al. 2014; Logerwell et al. 2015). Mean winds on the Beaufort shelf are westward year-round and westward flow over the shelf can transport water into Barrow Canyon (Weingartner et al. 2017), along with developing eggs and larvae inhabiting Beaufort shelf waters. During periods of weak winds, a strong shelf-break front forms along the southeastern edge of Barrow Canyon when the shelf-break currents flow onto the Beaufort shelf or along the canyon edge, which promotes the aggregation and retention of plankton on the western Beaufort Shelf (Okkonen et al. 2011). Barrow Canyon is a known biological "hotspot," with elevated nutrient concentrations, enhanced productivity rates, high benthic biomass, and high concentrations of seabirds and marine mammals (Grebmeier et al. 2015; Kuletz et al. 2015). Thus, it is likely that changing wind and current patterns, along with the shelf-break front, play an important role in the retention of gadid ELS around Barrow Canyon, which may provide them with enhanced feeding opportunities in these highly productive waters. Small polar cod larvae were also found east of Wrangel Island in the western Chukchi Sea and around Hanna Shoal on the northern Chukchi shelf, which suggests that these areas may also be important for spawning and retention. Kono et al. (2016) have suggested the presence of two separate spawning areas in the northern Bering and Chukchi seas. The presence of two separate populations is also supported by two separate high-density "hotspots" for polar cod ELS off Cape Lisburne and in Barrow Canyon, respectively (Fig. 6).

Peak hatching of saffron cod occurs in April and May, with larvae spending between 2–3 months in the plankton before descending to the bottom in mid-summer (Wolotira 1985). As most sampling occurred in late summer, during August and September, saffron cod ELS are likely not well represented in the ichthyoplankton surveys, which could explain why few fish were collected. Additionally, young saffron cod are known to occupy shallow, nearshore areas (Pokrovskaya 1960; Logerwell et al. 2015). The surveys in this study did not sample nearshore habitats well, with the nearest stations in the ichthyoplankton and AT surveys located more than 3 and 7.5 km away from land, respectively. Alternatively, saffron cod may exhibit more avoidance behavior to trawl gear compared to polar cod (see De Robertis et al. 2017a, their Fig. 9a, b). Thus, relationships between environmental drivers and saffron cod abundance in their nursery habitats are not fully resolved by this analysis, although higher abundances are strongly linked to higher temperatures.

While mature polar cod and saffron cod in spawning condition have been observed in the coastal waters of the Chukchi and Beaufort seas (Craig et al. 1982; Wolotira 1985), major spawning locations have not been identified.

Barrow Canyon and/or the surrounding waters may be potential candidates, given that small larvae were abundant in ichthyoplankton samples collected in the vicinity. Currently, minimal sampling has occurred in the region outside of the summer months, thus our knowledge about the seasonal distribution and abundance of these species is extremely limited, particularly during the spawning and hatching seasons. Earlier and more frequent sampling, including sampling during winter months, can help to identify spawning locations and habitat important to developing ELS. In June 2017 and 2018, the Arctic Shelf Growth, Advection, Respiration, and Deposition Rate Experiment (ASGARD) survey conducted process studies of oceanography and lower trophic levels in the northern Bering and southern Chukchi seas. This research will provide additional insights into the late spring distributions of polar cod and saffron cod ELS in the region. Preliminary findings indicate that small, age-0 gadids were highly abundant in Bongo net samples collected in nearshore waters (B. Norcross, University of Alaska Fairbanks, personal communication). To date, information about the vertical distributions of polar cod ELS in the water column is limited to a few studies (Borkin et al. 1986; Lafrance 2009; Bouchard et al. 2016), but is lacking for saffron cod. Depth-discrete sampling would provide important information on the vertical distributions of the different ontogenetic stages. Increased sampling in the nearshore region may also reveal the extent to which it is used for spawning or as juvenile nursery habitat. Identifying major spawning locations of polar cod and saffron cod, resolving the movement and distribution of their ELS, and understanding their responses to variable environmental forcing cannot be accomplished through field sampling alone, but will require the use of biophysical models that can track and simulate the behavior of eggs and larvae. These types of models have been used with success to model growth, mortality, and habitat connectivity of polar cod around Greenland (Thanassekos and Fortier 2012; Thanassekos et al. 2012), and we are currently adapting a model developed for walleye pollock (Petrik et al. 2015, 2016) to simulate the dispersal of polar cod and saffron cod in the Pacific Arctic. These models will provide valuable information about spawning, growth, and potential habitat use of these species. Echosounders moored on the seafloor will also provide information about the seasonal dynamics and movements of these fishes, as well as their zooplankton prey (Kitamura et al. 2017; De Robertis et al. 2018).

The goal of this research was to improve our knowledge about polar cod and saffron cod ELS by using available field data to characterize their distribution and abundance in the Pacific Arctic. Our study synthesized much of the available information on the distribution of their ELS from ichthyoplankton surveys that took place in the region between 2004 and 2013 and re-analyzed existing AT survey data to examine the distribution and abundance of fish across three ELS. Species- and stage-specific differences in habitat use were found, with polar cod having a more offshore and northern distribution compared to saffron cod, which were found closer inshore and farther south. Polar cod preflexion and flexion larvae were found throughout the sampling season in Bongo net samples across much of the Chukchi shelf, which suggests that spawning occurs over several months and at multiple locations, with Barrow Canyon potentially serving as an important spawning and/or retention area. Changes in depth, temperature, and salinity differentially affected the abundance of polar cod and saffron cod ELS. Environmental associations varied between years, and to a lesser extent, among developmental stages. This study provides important baseline information about the distribution and abundance of polar cod and saffron cod ELS in Alaska's Arctic and how they respond to environmental variability. Results of this study can be used to help describe EFH, which is currently undefined for ELS in Arctic waters, and can be used to help inform IBMs developed to identify polar cod and saffron cod spawning locations and source/sink populations. By identifying habitats important to polar cod and saffron cod ELS and the factors that influence their distribution and abundance in these habitats, we can better understand how these ecologically important species may respond to a changing environment, leading to more effective management of their populations under anticipated warming and increased human development in the Arctic.

Acknowledgements This study was supported by a grant from the North Pacific Research Board (Project #1508) and was also funded in part by the Bureau of Ocean and Energy Management (BOEM) Award # M12AC00009 and in part with qualified outer continental shelf oil and gas revenues by the Coastal Impact Assistance Program, U.S. Fish and Wildlife Service, U.S. Department of the Interior (Contracts #s: 10-CIAP-010; F12AF00188). This paper is EcoFOCI Contribution No. EcoFOCI-N911. The authors wish to thank the scientists and volunteers that collected data on the AFSC, RUSALCA, and Arctic Eis surveys. We would also like to thank Benjamin Laurel, Alison Deary, and 2 independent reviewers for their helpful comments on this manuscript. The findings and conclusions in this paper are those of the authors and do not necessarily represent the views of the National Marine Fisheries Service. Mention of trade names does not imply endorsement by NOAA or any of its subagencies.

Compliance with ethical standards

Conflict of interest The authors declare that they have no conflict of interest.

References

Aagaard K, Weingartner TJ, Danielson SL, Woodgate RA, Johnson GC, Whitledge TE (2006) Some controls on flow and salinity in Bering Strait. Geophys Res Lett 33:L19602

Abookire AA, Piatt JF, Robards MD (2000) Nearshore fish distributions in an Alaskan estuary in relation to stratification, temperature and salinity. Estuar Coast Shelf Sci 51:45–59

Akaike H (1998) Information theory and an extension of the maximum likelihood principle. In: Parzen E, Tanabe K, Kitagawa G (eds) Selected papers of Hirotugu Akaike. Springer, New York, pp 199–213

Altukhov KA (1981) The reproduction and development of the arctic cod, *Boreogadus saida*, in the White Sea. J Ichthyol 19:93–101

Aronovich TM, Doroshev SI, Spectorova LV, Makhotin VM (1975) Egg incubation and larval rearing of navaga (*Eleginus navaga* Pall.), polar cod (*Boreogadus saida* Lepechin) and arctic flounder (*Liopsetta glacialis* Pall.) in the laboratory. Aquaculture 6:233–242

Bailey KM, Houde ED (1989) Predation on eggs and larvae of marine fishes and the recruitment problem. Adv Mar Biol 25:1–83

Bailey KM, Picquelle SJ (2002) Larval distribution of offshore spawning flatfish in the Gulf of Alaska: potential transport pathways and enhanced onshore transport during ENSO events. Mar Ecol Prog Ser 236:205–217

Bailey KM, Nakata H, Van der Veer HW (2005) The planktonic stages of flatfishes: physical and biological interactions in transport processes. In: Gibson RN (ed) Flatfishes: biology and exploitation. Blackwell Science, Oxford, pp 94–119

Bailey KM, Abookire AA, Duffy-Anderson JT (2008) Ocean transport paths for the early life history stages of offshore spawning flatfishes: a case study in the Gulf of Alaska. Fish Fish 91:44–66

Baranenkova AS, Ponomarenko VP, Khokhlina NS (1966) The distribution, size and growth of the larvae and fry of *Boreogadus saida* (Lep.) in the Barents Sea. Fish Mar Serv Transl Ser 4025:498–518

Benoit D, Simard Y, Fortier L (2014) Pre-winter distribution and habitat characteristics of polar cod (*Boreogadus saida*) in southeastern Beaufort Sea. Polar Biol 37:149–163

Berg LS (1949) Ryby presnykh vod SSSR i sopredel'nykh stran (Freshwater Fishes of the USSR and Adjacent Countries). Zoological Institute of the Academy of Sciences of the USSR, USSR, Leningrad (in Russian)

Bond WA (1982) Study of the fishery resources of Tuktoyaktuk harbour, Southern Beaufort Sea Coast, with special reference to life histories of anadromous Coregonids. Can Tech Rep Fish Aquat Sci 1:1–19

Borkin LV, Ozhigin VK, Shleinik VN (1986) Effect of oceanographical factors on the abundance of the Barents Sea polar cod year classes. In: The effect of oceanographic conditions on distribution and population dynamics of commercial fish stocks in the Barents Sea, vol. 169

Bouchard C, Fortier L (2008) Effects of polynyas on the hatching season, early growth and survival of polar cod *Boreogadus saida* in the Laptev Sea. Mar Ecol Prog Ser 355:247–256

Bouchard C, Fortier L (2011) Circum-arctic comparison of the hatching season of polar cod *Boreogadus saida*: a test of the freshwater winter refuge hypothesis. Prog Oceanogr 90:105–116

Bouchard C, Mollard S, Suzuki K, Robert D, Fortier L (2016) Contrasting the early life histories of sympatric Arctic gadids *Boreogadus saida* and *Arctogadus glacialis* in the Canadian Beaufort Sea. Polar Biol 39:1005–1022

Bouchard C, Geoffroy M, LeBlanc M, Majewski A, Gauthier S, Walkusz W, Reist JD, Fortier L (2017) Climate warming enhances polar cod recruitment, at least transiently. Prog Oceanogr 156:121–129

Bradstreet MS (1986) Aspects of the biology of Arctic cod (*Boreogadus saida*) and its importance in Arctic marine food chains. Department of Fisheries and Oceans, Central and Arctic Region

Coachman LK, Aagaard K, Tripp RB (1975) Bering Strait: the regional physical oceanography. University of Washington Press, Seattle

Comiso JC, Parkinson CL, Gersten R, Stock L (2008) Accelerated decline in the Arctic sea ice cover. Geophys Res Lett 35:L01703

Copeman LA, Laurel BJ, Boswell KM, Sremba AL, Klinck K, Heintz RA, Vollenweider JJ, Helser TE, Spencer ML (2016) Ontogenetic and spatial variability in trophic biomarkers of juvenile saffron cod (*Eleginus gracilis*) from the Beaufort, Chukchi and Bering Seas. Polar Biol 39:1109–1126

Copeman LA, Laurel BJ, Spencer M, Sremba A (2017) Temperature impacts on lipid allocation among juvenile gadid species at the Pacific Arctic-Boreal interface: an experimental laboratory approach. Mar Ecol Prog Ser 566:183–198

Corlett WB, Pickart RS (2017) The Chukchi slope current. Prog Oceanogr 153:50–65

Craig PC, Haldorson L (1981) Beaufort Sea barrier island-lagoon ecological process studies: final report, Simpson Lagoon. Part 4. Fish. In: Environmental assessment of the Alaskan continental shelf. Final reports of principal investigators, vol 7, pp 384–678

Craig PC, Griffiths WB, Haldorson L, McElderry H (1982) Ecological studies of Arctic Cod (*Boreogadus saida*) in Beaufort Sea coastal waters. Can J Fish Aquat Sci 39:395–406

Danielson SL, Eisner L, Ladd C, Mordy C, Sousa L, Weingartner TJ (2017) A comparison between late summer 2012 and 2013 water masses, macronutrients, and phytoplankton standing crops in the northern Bering and Chukchi Seas. Deep Sea Res Part II 135:7–26

De Robertis A, Taylor K, Williams K, Wilson CD (2017a) Species and size selectivity of two midwater trawls used in an acoustic survey of the Alaska Arctic. Deep Sea Res Part II 135:40–50

De Robertis A, Taylor K, Wilson C, Farley E (2017b) Abundance and distribution of Arctic cod (*Boreogadus saida*) and other pelagic fishes over the US Continental Shelf of the Northern Bering and Chukchi Seas. Deep Sea Res Part II 135:51–65

De Robertis A, Levine R, Wilson C (2018) Can a bottom-moored echosounder array provide a survey-comparable index of abundance? Can J Fish Aquat Sci 75:629–640

Duffy-Anderson JT, Bailey KM, Cabral HN, Nakata H, Van der Veer HW (2014) The planktonic stages of flatfishes: physical and biological interactions in transport processes. In: Gibson RN (ed) Flatfishes: biology and exploitation. Blackwell Science, Oxford, pp 132–170

Eisner L, Hillgruber N, Martinson E, Maselko J (2012) Pelagic fish and zooplankton species assemblages in relation to water mass characteristics in the northern Bering and southeast Chukchi seas. Polar Biol 36:87–113

ESRI (2017) ArcGIS desktop: release 10.4. Environmental Systems Research Institute, Redlands

Fechhelm, RG, Craig, PC, Baker, JS, Gallaway, BJ (1985) Fish distribution and use of nearshore waters in the northeastern Chukchi Sea. In: US Department of Commerce, NOAA, and US Department of the Interior, Minerals Management Service, Outer Continental Shelf Environmental Assessment Program final report, vol 32, pp 121–298

Fortier L, Sirois P, Michaud J, Barber D (2006) Survival of arctic cod larvae (*Boreogadus saida*) in relation to sea ice and temperature in the Northeast Water Polynya (Greenland Sea). Can J Fish Aquat Sci 63:1608–1616

Geoffroy M, Robert D, Darnis G, Fortier L (2011) The aggregation of polar cod (*Boreogadus saida*) in the deep Atlantic layer of ice-covered Amundsen Gulf (Beaufort Sea) in winter. Polar Biol 34:1959–1971

Gjøsæter J (1973) Preliminary results of Norwegian polar cod investigations 1970-1972. ICES, Denmark

Graham M, Hop H (1995) Aspects of reproduction and larval biology of Arctic Cod (*Boreogadus saida*). Arctic 48:130–135

Grebmeier JM, Bluhm BA, Cooper LW, Danielson SL, Arrigo KR, Blanchard AL, Clarke JT, Day RH, Frey KE, Gradinger RR, Kędra M (2015) Ecosystem characteristics and processes facilitating persistent macrobenthic biomass hotspots and associated benthivory in the Pacific Arctic. Prog Oceanogr 136:92–114

Guisan A, Edwards TC Jr, Hastie T (2002) Generalized linear and generalized additive models in studies of species distributions: setting the scene. Ecol Model 157:89–100

Hastie TJ, Tibshirani RJ (1990) Generalized additive models. Chapman & Hall/CRC, London

Heintz RA, Siddon EC, Farley EA Jr, Napp JM (2013) Climate related changes in the nutritional condition of young-of-the year walleye pollock (*Theragra chalcogramma*) from the eastern Bering Sea. Deep Sea Res Part II 94:150–156

Helser TE, Colman JR, Anderl DM, Kastelle CR (2017) Growth dynamics of saffron cod (*Eleginus gracilis*) and Arctic cod (*Boreogadus saida*) in the Northern Bering and Chukchi Seas. Deep Sea Res Part II 135:66–77

ICES CM (1983) Preliminary report of the international 0-group fish survey in the Barents Sea and adjacent waters in August-September 1983. In: ICES Council Meeting

ICES CM (1985) Preliminary report of the international 0-group fish survey in the Barents Sea and adjacent waters in August-September 1985. In: ICES Council Meeting

ICES CM (1986) Preliminary report of the international 0-group fish survey in the Barents Sea and adjacent waters in August-September 1986. In: ICES Council Meeting

ICES CM (1987) Preliminary report of the international 0-group fish survey in the Barents Sea and adjacent waters in August-September 1987. In: ICES Council Meeting

ICES CM (1988) Preliminary report of the international 0-group fish survey in the Barents Sea and adjacent waters in August-September 1988. In: ICES Council Meeting

Ichthyoplankton Information System (2018) National Oceanic and Atmospheric Administration. https://access.afsc.noaa.gov/ichthyo/index.php. Accessed 14 April 2016

Iles TD, Sinclair M (1982) Atlantic herring: stock discreteness and abundance. Science 215:627–633

Johnson JJ (1995) Description and comparison of two populations of Saffron Cod (*Eleginus gracilis*) from Western Canadian Arctic Coastal Waters. Thesis, University of Manitoba

Kitamura M, Amakasu K, Kikuchi T, Nishino S (2017) Seasonal dynamics of zooplankton in the southern Chukchi Sea revealed from acoustic backscattering strength. Cont Shelf Res 133:47–58

Koenker B, Laurel BJ, Copeman LA, Ciannelli L (2018) Effects of temperature and food availability on the survival and growth of larval Arctic cod (*Boreogadus saida*) and walleye pollock (*Gadus chalcogrammus*). ICES J Mar Sci 75:2386–2402

Kono Y, Sasaki H, Kurihara Y, Fujiwara A, Yamamoto J, Sakurai Y (2016) Distribution pattern of Polar cod (*Boreogadus saida*) larvae and larval fish assemblages in relation to oceanographic parameters in the northern Bering Sea and Chukchi Sea. Polar Biol 39:1039–1048

Kuletz KJ, Ferguson MC, Hurley B, Gall AE, Labunski EA, Morgan TC (2015) Seasonal spatial patterns in seabird and marine mammal distribution in the eastern Chukchi and western Beaufort seas: Identifying biologically important pelagic areas. Prog Oceanogr 136:175–200

Ladd C, Mordy CW, Salo SA, Stabeno PJ (2016) Winter water properties and the Chukchi Polynya. J Geophys Res Oceans 121:5516–5534

Lafrance P (2009) Saison d'éclosion et survie des stades larvaires et juvéniles chez la morue arctique (*Boreogadus saida*) du sud-est de la mer de Beaufort. Dissertation. Université Laval

Laprise R, Pepin P (1995) Factors influencing the spatio-temporal occurrence of fish eggs and larvae in a northern, physically dynamic coastal environment. Mar Ecol Prog Ser 15:73–92

Laurel BJ, Spencer M, Iseri P, Copeman LA (2016) Temperature-dependent growth and behavior of juvenile Arctic cod (*Boreogadus saida*) and co-occurring North Pacific gadids. Polar Biol 39:1127–1135

Laurel BJ, Copeman LA, Spencer M, Iseri P (2017) Temperature-dependent growth as a function of size and age in juvenile Arctic cod (*Boreogadus saida*). ICES J Mar Sci 74:1614–1621

Litvak MK, Leggett WC (1992) Age and size-selective predation on larval fishes: the bigger-is-better hypothesis revisited. Mar Ecol Prog Ser 81:13–24

Logerwell E, Busby M, Carothers C, Cotton S, Duffy-Anderson J, Farley E, Goddard P, Heintz R, Holladay B, Horne J, Johnson S (2015) Fish communities across a spectrum of habitats in the western Beaufort Sea and Chukchi Sea. Prog Oceanogr 136:115–132

Marsh JM, Mueter FJ, Iken K, Danielson S (2017) Ontogenetic, spatial and temporal variation in trophic level and diet of Chukchi Sea fishes. Deep Sea Res Part II 135:78–94

Matarese AC, Kendall AW, Blood DM, Vinter BM (1989) Laboratory guide to early life history stages of northeast Pacific fishes. U.S. National Archives and Records Administration, College Park

Mecklenburg CW, Mecklenburg TA, Thorsteinson LK (2002) Fishes of Alaska. American Fisheries Society, Bethesda

Mecklenburg CW, Lynghammar A, Johannesen E, Byrkjedal I, Christiansen JS, Dolgov AV, Karamushko OV, Møller PR, Steinke D, Wienerroither RM (2018) Marine fishes of the Arctic region, vol 2. Conservation of Arctic Flora and Fauna, Akureyri

Miller TJ, Crowder LB, Rice JA, Marschall EA (1988) Larval size and recruitment mechanisms in fishes: toward a conceptual framework. Can J Fish Aquat Sci 45(9):1657–1670

Moore SE, Stabeno PJ (2015) Synthesis of Arctic Research (SOAR) in marine ecosystems of the Pacific Arctic. Prog Oceanogr 136:1–11

Morrow JE (1980) The freshwater fishes of Alaska. Alaska Northwest Publishing Company, Anchorage

Moskalenko BF (1964) O biologii polyarnoi treski (saiki) Boreogadus saida (Lepechin).[On the biology of the polar cod (*Boreogadus saida*).]. Vogr.| khtiol 4:435-443

Moulton LL, Tarbox KE (1987) Analysis of Arctic cod movements in the Beaufort Sea nearshore region 1978-79. Arctic 40:43-49

Mueter FJ, Weems J, Farley EV, Sigler MF (2017) Arctic ecosystem integrated survey (Arctic Eis): marine ecosystem dynamics in the rapidly changing Pacific Arctic Gateway. Deep Sea Res Part II 135:1–6

National Ice Center/Naval Ice Center Daily Ice Analysis Products, Ice Edge. https://www.natice.noaa.gov/products/daily_products.html. Accessed 20 Oct 2016

National Snow and Ice Data Center. Compiled by F. Fetterer, M. Savoie, S. Helfrich, and P. Clemente-Colón. 2010, updated daily. Multisensor Analyzed Sea Ice Extent - Northern Hemisphere (MASIE-NH), version 1. NSIDC: National Snow and Ice Data Center, Boulder. https://doi.org/10.7265/N5GT5K3K. Accessed 30 September 2016

Nikolayev AV, Kuznetsov MY, Syrovatkin EV (2008) Acoustic research of Arctic cod (*Boreogadus saida*) in the Bering and Chukchee Seas (Russian EEZ) in 1999–2007. Izv. TINRO 155:131–143

Nikolski GV (1954) Chastnaya ikhtiologiya (Speciat Ichthyology). Israel Program for Scientific Translations, Israel

Norcross BL, Holladay BA, Busby MS, Mier KL (2010) Demersal and larval fish assemblages in the Chukchi Sea. Deep Sea Res Part II 57:57–70

Okkonen SR, Ashjian CJ, Campbell RG, Clarke JT, Moore SE, Taylor KD (2011) Satellite observations of circulation features associated with a bowhead whale feeding 'hotspot' near Barrow, Alaska. Remote Sens Environ 115:2168–2174

Parker-Stetter SL, Horne JK, Weingartner TJ (2011) Distribution of polar cod and age-0 fish in the US Beaufort Sea. Polar Biol 34:1543–1557

Petrik CM, Duffy-Anderson JT, Mueter F, Hedstrom K, Curchitser EN (2015) Biophysical transport model suggests climate variability determines distribution of Walleye Pollock early life stages in the eastern Bering Sea through effects on spawning. Prog Oceanogr 138:459–474

Petrik CM, Duffy-Anderson JT, Castruccio F, Curchitser EN, Danielson SL, Hedstrom K, Mueter F (2016) Modelled connectivity between Walleye Pollock (*Gadus chalcogrammus*) spawning and age-0 nursery areas in warm and cold years with implications for juvenile survival. ICES J Mar Sci 73:1890–1900

Pokrovskaya TN (1960) Geograficheskaya izmenchivost' biologii navagi (roda *Eleginus*) (Geographical variability in the biology of the navaga (genus *Eleginus*)). Trudy Inst Okeanol 31:19–110

Ponomarenko VP (1967) Feeding of the larvae and fry of the Arctic Cod (*Boreogadus saida* Lepechin) in the Barents and Kara seas. Materialy Rybokhozyaistvennykh Issledovanii Severnogo Basseina, Vypusk X, Ministerstvo Rybnogo Khozyaistva SSSR, Polyarnyi Nauchno-Issledovaltel'skii i Proektnyi Institut Morskogo Rybnogo Khozyaistva i Okeanografii Im. NM Knipovicha (PINRO) 10:20–27

Ponomarenko VP (1968) Some data on the distribution and migrations of polar cod in the seas of the Soviet Arctic. Rapp PV Reun Cons Perm Int Explor Mer 158:131–135

Ponomarenko VP (2000) Eggs, larvae, and juveniles of polar cod *Boreogadus saida* in the Barents, Kara, and White Seas. J Ichthyol 40:165–173

R Core Team (2017) R: a language and environment for statistical computing. R Foundation for Statistical Computing, Vienna

Rajasakaren B (2013) Distribution of polar cod (*Boreogadus saida*) in the Barents Sea: a useful indicator of climate variation. University of Bergen, Thesis

Rass TS (1968) Spawning and development of polar cod. Rapp PV Reun Cons Perm Int Explor Mer 158:135–137

Richter-Menge J, Overland JE, Mathis JT (2016) Arctic report card, ftp://ftp.oar.noaa.gov/arctic/documents/arcticreportcard_full_report2016.pdf. Accessed 27 October 2017

Sakurai Y, Ishii K, Nakatani T, Yamaguchi H, Anma G, Jin M (1998) 15. Reproductive characteristics and effects of temperature and salinity on the development and survival of eggs and larvae of arctic cod (*Boreogadus saida*). Mem Fac Fish Hokkaido Univ 45:77–89

Sambrotto RN, Goering JJ, McRoy CP (1984) Large yearly production of phytoplankton in the western Bering Strait. Science 225:1147–1150

Scott WB, Scott MG (1988) Atlantic fishes of Canada. University of Toronto Press, Toronto

Shleinik VN (1973) The state of stock and perspectives of polar cod fishery in the Barents Sea. Tr Polyarn Inst Morsk Rybn Khoz Okeanogr 33:225–235

Shono H (2008) Application of statistical modeling and data mining method to the fish stock analyses. Bull Fish Res Agen 22:1–85

Stammerjohn S, Massom R, Rind D, Martinson D (2012) Regions of rapid sea ice change: an inter-hemispheric seasonal comparison. Geophys Res Lett 39:L05502

Stigebrandt A (1984) The North Pacific: a global-scale estuary. J Phys Oceanogr 14:464–470

Sunnanå K, Christiansen JS (1997) Kommersielt fiske på polar torsk–erfaringer og potensiale. Fiskeriforsknings Rapportserie 1:20

Thanassekos S, Robert D, Fortier L (2012) An individual based model of Arctic Cod (*Boreogadus saida*) early life in Arctic polynyas: II. Length-dependent and growth-dependent mortality. J Mar Syst 93:39–46

Thanassekos S, Fortier L (2012) An individual based model of Arctic cod (*Boreogadus saida*) early life in Arctic polynyas: I. Simulated growth in relation to hatch date in the Northeast Water (Greenland Sea) and the North Water (Baffin Bay). J Mar Syst 93:25–38

Tweedie MC (1957) Statistical properties of inverse gaussian distributions. I. Ann Math Stat 28:362–377

U.S. Sustainable Fisheries Act (1996) Report of the committee on commerce, science, and transportation on S.39: Sustainable Fisheries Act Report 104-276, 104th Congress, Second Session, US Senate 23 May 1996. US Government Printing Office, Washington, DC

Vasil'kov VP, Chupysheva NG, Kolesova NG (1981) The possibility of long-term forecasting from solar activity cycles of catches of the Saffron cod, *Eleginus gracilis*, in the Sea of Japan. J Ichthyol 22:26–33

Weingartner T, Aagaard K, Woodgate R, Danielson S, Sasaki Y, Cavalieri D (2005) Circulation on the north central Chukchi Sea shelf. Deep Sea Res Part II 52:3150–3174

Weingartner TJ, Potter RA, Stoudt CA, Dobbins EL, Statscewich H, Winsor PR, Mudge TD, Borg K (2017) Transport and thermohaline variability in Barrow Canyon on the Northeastern Chukchi Sea Shelf. J Geophys Res Oceans 122:3565–3585

Weingartner TJ (1997) A review of the physical oceanography of the northeastern Chukchi Sea. In: Reynolds JB (ed) Fish ecology in Arctic North America. American Fisheries Society Symposium 19. American Fisheries Society, Bethesda, pp 40-59

Whitehouse GA (2011) Modeling the Eastern Chukchi sea food web with a mass-balance approach. Doctoral dissertation, University of Washington

Winker H, Kerwath SE, Attwood CG (2014) Proof of concept for a novel procedure to standardize multispecies catch and effort data. Fish Res 155:149–159

Wolotira RJ Jr (1985) Saffron cod (*Eleginus gracilis*) in western Alaska: the resource and its potential. Northwest and Alaska Fisheries Center, Kodiak

Wood SN (2003) Thin plate regression splines. J R Stat Soc Ser B 65:95–114

Wood SN (2004) Stable and efficient multiple smoothing parameter estimation for generalized additive models. J Am Stat Assoc 99:637–686

Wood SN (2006) Generalized additive models: an introduction with R. Chapman & Hall/CRC, Boca Raton

Wood KR, Bond NA, Danielson SL, Overland JE, Salo SA, Stabeno PJ, Whitefield J (2015) A decade of environmental change in the Pacific Arctic region. Prog Oceanogr 136:12–31

Woodgate RA, Aagaard K, Weingartner TJ (2005) Monthly temperature, salinity, and transport variability of the Bering Strait through flow. Geophys Res Lett 32:L04601

Wyllie-Echeverria T, Barber WE, Wyllie-Echeverria S (1997) Water masses and transport of age-0 Arctic Cod and age-0 Bering flounder into the northeastern Chukchi Sea. In: Reynolds JB (ed) Fish ecology in Arctic North America. American Fisheries Society Symposium 19. American Fisheries Society, Bethesda, pp 60–67

Yudanov IG (1976) Zoogeography of polar cod in the Arctic Ocean. Priroda i Khoziaistvo Severa (Nature and Economy of the North), vol 4. KNTs RAN, Apatity, pp 111–113